Inorganic Chemistry

Article

pubs.acs.org/IC

Li/X Phosphinidenoid Pentacarbonylmetal Complexes: A Combined Experimental and Theoretical Study on Structures and Spectroscopic Properties

Rainer Streubel,*[,†] Aysel Özbolat-Schön,[†] Gerd von Frantzius,[†] Holly Lee,[‡] Gregor Schnakenburg,[†] and Dietrich Gudat[§,∥]

[†]Institut für Anorganische Chemie, Rheinische Friedrich-Wilhelms-Universität Bonn, Gerhard-Domagk-Strasse 1, 53121 Bonn, Germany

[‡]Department of Chemistry, University of Toronto, 80 St. George Street, Room 321A, M5S 3H6 Toronto, Ontario, Canada

[§]Institut für Anorganische Chemie, Universität Stuttgart, Pfaffenwaldring 55, Stuttgart, Germany

Supporting Information

ABSTRACT: The synthesis of *P*-F phosphane metal complexes $[(CO)_5M\{RP(H)F\}]$ **2a−c** (R = $CH(SiMe_3)_2$; **a**: M = W; **b**: M = Mo; **c**: M = Cr) is described using $AgBF_4$ for a Cl/F exchange in *P*-Cl precursor complexes $[(CO)_5M\{RP(H)Cl\}]$ **3a−c**; thermal reaction of 2*H*-azaphosphirene metal complexes $[(CO)_5M\{RP(C(Ph)=N\}]$ **1a−c** with $[Et_3NH]X$ led to complexes **3a−c**, **4**, and **5** (M = W; **a−c**: X = Cl; **4**: X = Br; **5**: X = I). Complexes **2a−c**, **3a−c**, **4**, and **5** were deprotonated using lithium diisopropylamide in the presence of 12-crown-4 thus yielding Li/X phosphinidenoid metal complexes $[Li(12\text{-crown-}4)(Et_2O)_n][(CO)_5M(RPX)]$ **6a−c**, **7a−c**, **8**, and **9** (**6a−c**: M = W, Mo, Cr; X = F; **7a−c**: M = W, Mo, Cr; X = Cl; **8**: M = W; X = Br; **9**: M = W; X = I). This first comprehensive study on the synthesis of the title compounds reveals metal and halogen dependencies of NMR parameters as well as thermal stabilities of **6a**, **7a**, **8**, and **9** in solution (F > Cl > Br > I). DOSY NMR experiments on the Li/F phosphinidenoid metal complexes (**6a−c**; M = W, Mo, Cr) rule out that the cation and anion fragments are part of a persistent molecular complex or tight ion pair (in solution). The X-ray structure of **6a** reveals a salt-like structure of $[Li(12\text{-crown-}4)Et_2O][(CO)_5W\{P(CH(SiMe_3)_2)F\}]$ with long P−F and P−W bond distances compared to **2a**. Density functional theory (DFT) calculations provide additional insight into structures and energetics of cation-free halophosphanido chromium and tungsten complexes and four contact ion pairs of Li/X phosphinidenoid model complexes $[Li(12\text{-crown-}4)][(CO)_5M\{P(R)X\}]$ (**A-D**) that represent principal coordination modes. The significant increase of the compliance constant of the P−F bond in the anionic complex $[(CO)_5W\{P(Me)F\}]$ (**10a**) revealed that a formal lone pair at phosphorus weakens the P−F bond. This effect is further enhanced by coordination of lithium and/or the Li(12-crown-4) countercation (to **10a**) as in type **A-D** complexes. DFT calculated phosphorus NMR chemical shifts allow for a consistent interpretation of NMR properties and provide a preliminary explanation for the "abnormal" NMR shift of *P*-Cl derivatives **7a−c**. Furthermore, calculated compliance constants reveal the degree of P−F bond weakening in Li/F phosphinidenoid complexes, and it was found that a more negative phosphorus−fluorine coupling constant is associated with a larger relaxed force constant.

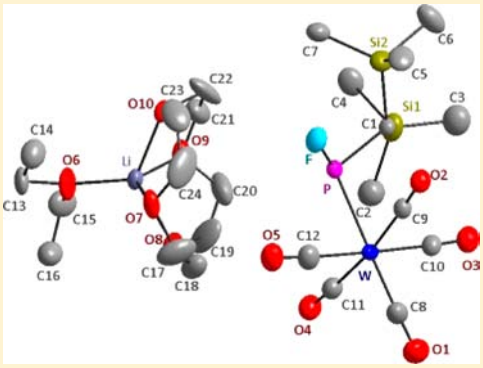

INTRODUCTION

Carbenoids[1,2] (**Ia**, E = C) as well as silylenoids[3−5] (**Ib**, E = Si, Scheme 1) are versatile compounds in organic synthesis. For example, they react as either nucleophiles or electrophiles and/or represent transfer agents of the corresponding transient carbene analogues if both philicities are operating cooperatively. The structures of such carbene-like species coined "enoids" usually possess elongated E-M and E-X bonds and distorted tetrahedral environments for the central atom E. An unusual structure of a Li/F silylenoid derivative **II** possessing lithium bound to fluorine and not the silicon center was reported by Apeloig and co-workers;[5] structurally confirmed examples for the inversely polarized type **III** are unknown. On the basis of density functional theory (DFT) calculations, another bonding mode and structure was proposed for silylenoids (**IV**)[4f] in which X and/or other atoms in the periphery of E may be involved in the bonding to M. Compared to carbenoids, silylenoids, and nitrenoids (**V**) (E = N), the chemistry of phosphinidenoids[6] (**V**) (Scheme 1) is not developed; the latter were only considered as intermediates. Besides thermochemical considerations, one might speculate at this point that the existence of a lone pair at phosphorus in **V** may facilitate reorganization, aggregation, and/or elimination, finally.

It should be noted that electrophilic terminal phosphinidene complexes with the general formula $L_nM(PR)$ have been

Received: December 21, 2012
Published: March 7, 2013

   dx.doi.org/10.1021/ic302786v | *Inorg. Chem.* 2013, 52, 3313−3325

Scheme 1. Carbenoids and Silylenoids (I–V), Phosphinidenoids (V), and Phosphinidenoid Complexes (VI) (E = main group elements, M = main group metals, L_nM = transition metal complexes, R^1,R^2 = organic substituents, X = halides)

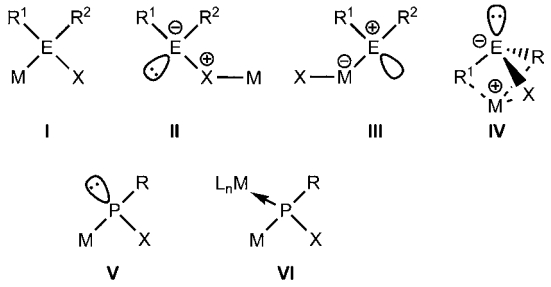

thoroughly studied for more than 30 years,[7] whereas bottleable phosphinidenes RP are still unknown;[8a,b] nevertheless, some phosphinidene-transfer reagents are available.[8c–f] The case of phosphinidenes impressively illustrates (once more) the concept of transition-metal stabilization of reactive intermediates. Consequent adaptation of this concept to the case of phosphinidenoids enabled to firmly establish Li/X phosphinidenoid tungsten complexes (**VI**, X = F,[9] Cl[10,11]) as a new class of highly reactive compounds in organophosphorus chemistry.[12] First studies on the reactivity of these species in solution had revealed nucleophilic reactivity in reactions with organic halides[10,11c,13] and terminal electrophilic phosphinidene complex-like behavior in reactions with π-substrates such as alkyne, carbonyl, and imine derivatives.[10,11c,14–16] As Li/X phosphinidenoid tungsten complexes **VI** also enable a facile entry to the chemistry of P-functional phosphanyl complexes,[17] we became even more interested to understand structural and physical properties of complexes **VI**.

Here, the first comprehensive study on synthesis and NMR spectroscopic data of a homologue series of Li/X phosphinidenoid metal complexes (M = Cr–W; X = F–I) is presented; DFT calculations provide a consistent interpretation of NMR properties. First insight into the bonding situation of these complexes in solution was obtained from DOSY experiments. Furthermore, the first-ever example of a single-crystal X-ray structure of a Li/X phosphinidenoid metal complex is reported.

RESULTS AND DISCUSSION

As previously demonstrated halogeno(organo)phosphane complexes enable access to Li/X phosphinidenoid complexes via *P*-H deprotonation[9–11] Therefore, we first synthesized complexes **3a**,[18] **3b,c** (X = Cl), **4**[19] (X = Br), and **5**[20] (X = I) using a selective thermal ring-cleavage reaction of 2*H*-azaphosphirene complexes **1a–c**[21] in the presence of triethylammonium halides (Scheme 2). Complex **5** was prepared using in situ formed $[Et_3NH]I$, obtained under typical 2*H*-azaphosphirene complex synthesis conditions while employing [bis(trimethylsilyl)-methylene]iodophosphane[22]and the appropriate aminocarbene complex, and heating of the resulting reaction solution. Reaction of *P*-Cl phosphane complexes **3a–c** with $AgBF_4$ then furnished selectively complexes **2a–c** (X = F) via chlorine/fluorine exchange reaction in **3a–c**.

All reactions, except the formation of **3b**, were highly selective and led to products that were obtained in good (**2a–c**: 70–85%, **3a**: 76%) or moderate (**3c**: 45%, **4**: 35%, **5**: 36%)

Scheme 2. Syntheses of *P*-X Phosphane Complexes 2a–c, 3a–c, 4, and 5

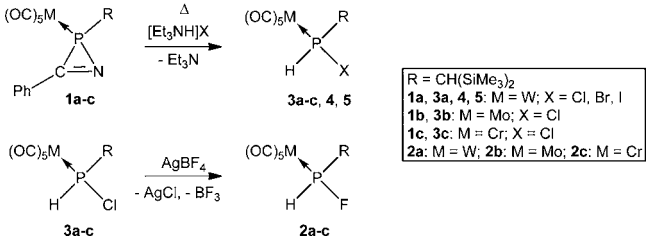

yields after purification by low temperature column chromatography; **3b** was obtained in low yields only (10%). Selected NMR-data of the new complexes will be discussed in the next paragraph (see Table 1).

Table 1. Comparison of ^{31}P NMR Data of 2a–c, 3a–c, 4, and 5 with 6a–c, 7a–c, 8, and 9

no.	$\delta(^{31}P)$	$^1J(W,P)$ [Hz]	$^1J(P,F)$ [Hz]	no.	$\delta(^{31}P)$	$^1J(W,P)$ [Hz]	$^1J(P,F)$ [Hz]
2a	154.2	286.1	806.2	**6a**[9]	305.9	71.3	614.6
2b	187.3		808.7	**6b**	343.9		605.3
2c	215.3		827.8	**6c**	353.0		665.0
3a	53.7	269.6		**7a**	212.9	67.4	
3b	88.9			**7b**	245.2		
3c	123.5			**7c**	274.7		
4	23.1	264.5		**8**	242.8	61.0	
5	−49.4	254.1		**9**	215.3	54.4	

All *P*-H phosphane complexes were then deprotonated using lithium diisopropylamide (LDA)[23] in $[D_8]$THF in the presence of 12-crown-4 at −78 °C, which led to a selective and complete conversion into the corresponding Li/X phosphinidenoid complexes **6a**,[9] **6b,c**, **7a–c**, **8**, and **9** (Scheme 3); all products were fully characterized by NMR spectroscopy at low temperature (for the ^{31}P NMR reaction monitoring of **6a** see the Supporting Information).

Scheme 3. Low Temperature Generation of *P*-bis(trimethylsilyl)methyl Substituted Li/X-Phosphinidenoid Complexes 6a–c, 7a–c, 8, and 9

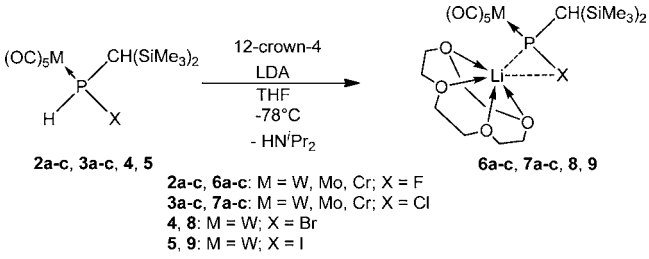

The $^{31}P\{^1H\}$ NMR spectra of the Li/F phosphinidenoid complexes **6a–c** disclose chemical shifts beyond 300 ppm (Table 1) which exceed the chemical shifts of the corresponding fluorophosphane complexes **2a–c** (δ = 150–215) by about 100–150 ppm. An increase in shielding within the triad chromium, molybdenum, and tungsten complexes is observed for *P*-F and *P*-Cl phosphane complexes (**2a–c** and **3a–c**) as well as the corresponding phosphinidenoid complexes (**6a–c** and **7a–c**).

dx.doi.org/10.1021/ic302786v | *Inorg. Chem.* 2013, 52, 3313–3325

The differences in ^{31}P NMR chemical shifts between the phosphane tungsten complexes **2a**, **3a**, **4**, and **5** and the corresponding phosphinidenoid complexes **6a**, **7a**, **8**, and **9** are similar for the fluorine and chlorine derivatives, but the additional deshielding of the phosphinidenoid complexes increases (relative to **7a**) for the bromine and iodine derivatives **8**, **9** (**8**: 242.8 ppm; **9**: 215.3 ppm). Furthermore, the ^{31}P chemical shifts of the Li/X phosphinidenoid complexes **6a**, **7a**, **8**, and **9** do not increase continuously with the metal atomic number as usually observed in many halogenophosphane complexes such as **2a**, **3a**, **4**, and **5**. Instead, the phosphorus nucleus experiences deshielding in going from the chlorine to the bromine derivative, and shielding when going from the bromine to the iodine derivative.[24] The most eye-catching feature of all tungsten phosphinidenoid complexes is the very low magnitude of ^{1}J(W,P), which is generally by some 200 Hz smaller than in the corresponding secondary halogenophosphane complexes (Table 1). The magnitude of ^{1}J(P,F)-coupling constants of fluoro complexes decreases from 805−828 Hz in **2a**−**c** to 614−665 Hz in **6a**−**c**.

While the $^{13}C\{^{1}H\}$ resonances of the carbon atom directly bonded to the phosphorus atom in complexes **6a**−**c** and **7a**−**c** are marginally deshielded when compared to the $^{13}C\{^{1}H\}$ resonances in complexes **2a**−**c** and **3a**−**c**, the magnitude of $^{1}J_{P,C}$ in the *P*-F and *P*-Cl substituted phosphinidenoid complexes (**6a**−**c**: 80−85 Hz, **7a**−**c**: 89−97 Hz) is by a factor of 5 to 10 larger than in the corresponding precursor complexes (**2a**−**c**: 19−28 Hz, **3a**−**c**: 5−10 Hz). Because of the absence of visible P−Li or F−Li couplings in complexes **6a**−**c**, the interaction of the lithium atom with the phosphorus and/or the fluorine atom remained unclear. To get more insight into the possible cation/anion interaction, solutions of these complexes were studied by diffusion ordered NMR spectroscopy (DOSY).

DOSY Experiments. Measurements were performed on samples of in situ prepared fluorophosphinidenoid complexes in a solvent mixture of THF-d_8 and 12-crown-4 and, for comparison, on a solution of phosphane complex **2a** and 12-crown-4. Whereas assignment of the ^{1}H, ^{19}F, and ^{31}P signals of **6a**−**c** in these solutions was unequivocal, the ^{7}Li NMR spectra revealed the presence of several species whose identification was not immediately evident. Measurement of a $^{1}H,^{7}Li$-HOESY spectrum sufficed, however, to assign the two major signals as those of $[Li(12\text{-cr-}4)]^{+}$ and an excess of metalating agent, $[Li(N^{i}Pr_2)]_x$, respectively. Chemical exchange between these species could not be detected by 2D-EXSY-experiments on a time scale of <66 ms. The ^{31}P NMR spectrum of molybdenum complex **6b** showed two lines with relative intensities of about 4:1 which display both the expected doublet splitting due to $^{1}J_{PF}$. This phenomenon may arise from a hindered rotation around the P−C bond thus giving rise to two atropisomers as it was detected recently for some oxaphosphirane complexes.[25] No temperature dependent line shape changes which might indicate dynamic exchange between two species were observed between −45 and −75 °C.

The diffusion coefficients calculated from different NMR signals are listed in Table 2. The data show clearly that the diffusion rates of cations and anions of complexes **6a**−**c** in the same solution exhibit significant differences. Although the comparison of diffusion coefficients between species in different samples is not straightforward (since small variations in the composition of the solvent mixture or different amounts of byproducts may induce perceptible variations in viscosities which in turn exerts a strong influence on the resulting value of *D*), the diffusion coefficients of the anionic fragments of **6a**−**c** are generally smaller than that of the fluorophosphane complex **2a**, which means in the context of the Stokes−Einstein equation that the hydrodynamic radii of the anions of complexes **6a**−**c** must be larger than that of **2a**.[26]

Table 2. Diffusion Coefficients *D* and Relative Radii *R* (with Respect to *R*(2a) = 1.0)

		$D \times 10^{10}$ [m^2/s]	R_{rel}[a] [Å]
complex **6a**	anion	1.35(7)	1.48
	cation	1.53(7)	1.31
complex **6b**	anion	1.5(1)	1.33
	cation	1.75	1.14
complex **6c**	anion	1.38(4)	1.45
	cation	1.57(5)	1.27
complex **2a**		2.0(1)	1.00
12-crown-4		3.4(1)	0.59

[a]Relative hydrodynamic ratio as calculated from the Stokes−Einstein equation.

Altogether, the results of the diffusion measurements allow us to rule out that the cation and anion fragments of **6a**−**c** are part of a persistent molecular complex or tight ion pair, and suggest that the complexes split up into separate cation and anion species which diffuse either independently from each other or exist in an equilibrium between a contact ion pair and a solvent separated ion pair.

Solid State Structure Determination. Single-crystals of complex **6a** suitable for X-ray diffraction analysis were obtained from the reaction solution (diethyl ether) after two weeks at −28 °C. The crystals contain a network of lithium cations, which coordinate a crown ether and an additional molecule of diethyl ether, and bis(trimethylsilyl)methyl(fluoro)-phosphanide unit coordinated to pentacarbonyltungsten (Figure 1). Weak hydrogen bonds connect the fluorine atom with two hydrogen atoms of $SiMe_3$ groups (H5A−F 2.59(1) Å, H7B−F 2.57(1) Å) and one hydrogen atom of 12-crown-4 (H24B−F 2.83(1) Å).

The phosphorus atom shows a pyramidal coordination sphere with a sum of bond angles of 306.7°, whereby the bond angles between phosphorus and adjacent atoms became smaller in case of phosphinidenoid complex **6a** compared to **2a**. Both the P−F (1.744(9) Å) and P−W bonds (2.580(3) Å) of **6a** are by some 0.14 Å longer than the corresponding bonds in complex **2a** (P−F 1.603(3) Å, P−W 2.4463(9) Å). A similar elongation of element-halogen bonds had also been noted for some carbenoids[27] and silylenoids,[5] and may thus be considered as a typical structural feature of these classes of compounds.

Computational Section. The theoretical knowledge about phosphinidenoids and their transition-metal complexes is scarce. Probably the first phosphinidenoid ever described by theory is lithium difluorophos-phinidenoid $LiPF_2$ which has according to MP2 calculations a bridged structure.[28] Furthermore, DFT calculations have been reported for the *P*-F phosphanido complex $[(CO)_5Cr\{P(Me)F\}]^{-}$[29] which was proposed as model for a nucleophilic tungsten complex supposedly formed in solution. Shortly afterward, DFT calculations were used to predict geometries, relative energies, and chemical shifts of different structural isomers of $[(CO)_5W(MePF)Li(12\text{-crown-}4)\}]$ in the gas phase). These studies led to the conclusion that a structure with a F−Li motif should be favored in solution.[9]

dx.doi.org/10.1021/ic302786v | *Inorg. Chem.* 2013, 52, 3313−3325

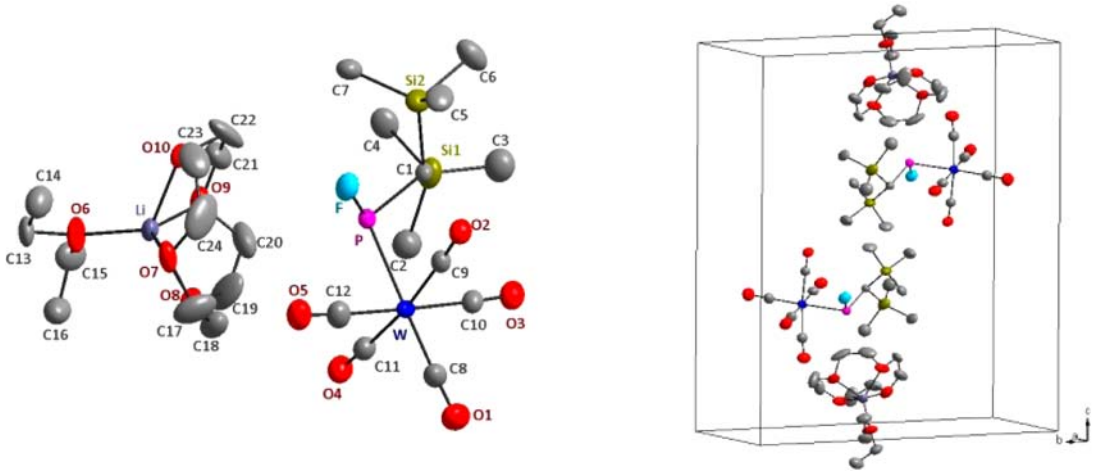

Figure 1. Molecular structure of complex **6a** in the crystal (20% probability level, hydrogen atoms are omitted for clarity). Top left: individual ion pair; top right: two enantiomeric ion pairs in the unit cell. Selected bond lengths [Å] and angles [deg]: W–P 2.580(3), P–C(1) 1.8402(1), P–F 1.744(9); W–P–C(1) 109.297(3), W–P–F 98.892(2), F–P–C(1) 98.470(3).

As the results of the DOSY experiments obtained in the present study as well as recent calculations on the molecular structures of a specific Li/Cl phosphinidenoid tungsten complex with a bulky CPh_3 substituent at phosphorus[11c] indicated that this conclusion is presumably wrong, a more detailed investigation using more refined structural models with inclusion of solvation effects seemed desirable.

We have therefore performed a broad computational study to compare DFT calculated structures and spectroscopic properties of cation-free ("naked") halophosphanido complexes $[(CO)_5M\{P(R)X\}]^-$ (M = Cr, Mo, W) with four basic types of Li/X phosphinidenoid complexes **A-D** (see Scheme 4). In the following discussion, we will focus mainly on tungsten complexes but additional informations on chromium and molybdenum complexes can be found in the Supporting Information. The four basic structure types **A-D** of phosphinidenoid complexes can be formally derived by considering further interaction of lithium derivatives **VII** and **VII′** with 12-crown-4 (**A-D**). In addition, the effect of microsolvation at lithium by Et_2O is considered in structural types **C*,D***.

Scheme 4. Halophosphanido Complexes $[(CO)_5M(PRX)]^-$, Two Isomeric Lithium Derivatives Thereof, $Li[(CO)_5M\{P(R)X\}]$ (Structure Types VII and VII′), and Four Basic Structure Types A-D of Lithium Phosphinidenoid Complexes [12-crown-4]$[(CO)_5M\{P(R)X\}]$, Including Et_2O in Isomers C*,D*

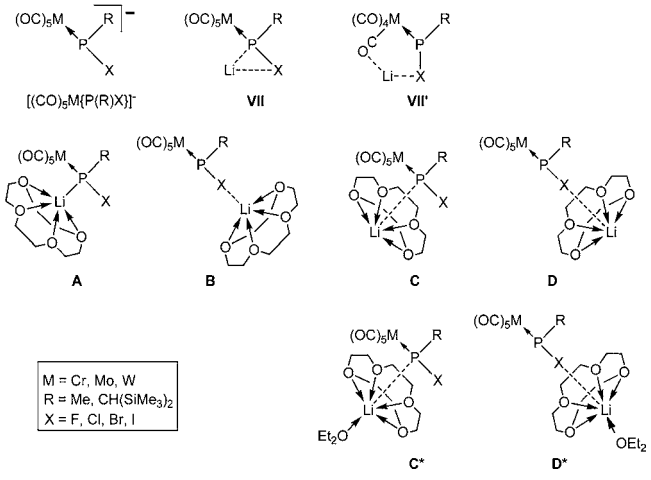

DFT Calculations. All optimizations and frequency calculations were performed using GAUSSIAN03/09[30] and ADF-2007.01/2009.01.[31] By default, DFT calculations with GAUSSIAN were carried out using the B3LYP[32] functional with 6-311G(d,p)[33] or Ahlrichs TZVP[34] basis sets for the light atoms and an effective core potential description using LanL2DZ by Hay and Wadt[35–37] for the heavy atoms. ADF calculations were carried out by default using the scalar relativistically corrected VWN[38]B[39]P86[40]/TZ2P SO ZORA method including spin–orbit correction (SO). Stationary points were characterized by analytical second derivatives. ^{31}P and ^{183}W NMR chemical shifts and nuclear spin–spin couplings were computed using ADFs SO ZORA GIAO–DFT method included in the CPL[41,37] module; calculated absolute isotropic shieldings for a species X were converted to common chemical shifts using the equations $\delta^{31}P(X) = \sigma(PH_3) - \sigma(X) - 266.1$[42] and $\delta^{183}W(X) = \sigma(W(CO)_6) - \sigma(X) - 3486$.[43a,44] Truhlar's recently proposed "continuum solvation model based on the quantum mechanical charge density of a solute" (SMD: IEFPCM(SMD)-B3LYP/TZVP) was used with the GAUSSIAN 09 defaults (e.g., van der Waals cavity, GePOL[45]) to calculate Gibbs energies of solvation. Truhlar's model is parametrized on a training set of neutral and ionic solutes in various solvents.[46] An obvious shortcoming of continuum models is the absence of any specific interaction of solvent and solute. In all cases to be treated here, this specific interaction is mimicked in the DFT treatment by including microsolvation of the lithium cation through coordination of a solvent moiety (Et_2O).

Halophosphanido and Lithium/Halo Phosphinidenoid Complexes. A series of *P*-Me and *P*-$CH(SiMe_3)_2$ substituted halophosphanido metal complexes was calculated to examine influences of the P-substituent onto structures and properties thus approaching the real system in the experiments step by step; information on the parent Li/F phosphinidenoid chromium complex can be found in the Supporting Information. Hereafter, the anionic complexes are presented first; bond lengths and angles of halophosphanido complexes $[(CO)_5M(PRX)]^-$, M = Cr (**10c**), Mo (**10b**), and W (**10a**,

dx.doi.org/10.1021/ic302786v | Inorg. Chem. 2013, 52, 3313–3325

11–**14**) are collected in Table 3 (gas phase at B3LYP/6-311g(d,p), LanL2DZ at M) and in Table 4 (M = Cr, R = Me,

Table 3. Bond Lengths [Å] of Halophosphanido Complexes $[(CO)_5M(PRX)]^-$ (10a-c, 11–14) at B3LYP/6-311g(d,p), LanL2DZ(M), M = Cr–W

	M	R	X	M–P [Å]	P–X [Å]	P–C [Å]	∑∠P [deg]
10c	Cr	Me	F	2.516	1.700	1.871	306.4
10b	Mo	Me	F	2.664	1.702	1.871	305.5
10a	W	Me	F	2.658	1.701	1.871	305.1
11	W	$CH(SiMe_3)_2$	F	2.686	1.720	1.909	311.3
12	W	$CH(SiMe_3)_2$	Cl	2.661	2.220	1.922	324.8
13	W	$CH(SiMe_3)_2$	Br	2.663	2.390	1.924	326.3
14	W	$CH(SiMe_3)_2$	I	2.664	2.632	1.927	328.8

Table 4. Bond Lengths [Å] of Halophosphanido Complexes $[(CO)_5Cr(PMeX)]^-$ (10c, 15, 16) at B3LYP/TZVP and, for Solution Phase Calculations, Truhlar's PCM-SMD Solution Model[46] at 298 K and 1 atm

	M	R	X	phase	Cr–P [Å]	P–X [Å]	P–C [Å]	∑∠P [deg]
10c	Cr	Me	F	gas	2.526	1.707	1.878	307.1
				Et_2O	2.506	1.722	1.869	307.4
15	Cr	Me	Cl	gas	2.528	2.213	1.882	310.1
				Et_2O	2.510	2.224	1.876	310.7
16	Cr	Me	Br	gas	2.527	2.387	1.884	311.2
				Et_2O	2.516	2.389	1.879	312.1

gas and solution phase at B3LYP/TZVP) (IR stretching frequencies are given in the Supporting Information). Somewhat counterintuitive was the finding that the longest tungsten–phosphorus bond was found for the gas phase structure of the fluorophosphanido complex $[(CO)_5W\{P(CH(SiMe_3)_2)F\}]^-$ (**11**) but this correlates well with the increasing steric demand of the *P*-$CH(SiMe_3)_2$ substituent if compared to the *P*-Me derivative **10a**.

The comparison between gas phase and (ethereal) solution structures for a set of *P*-Me model halophosphanido chromium complexes (X = F–Br) revealed that the phosphorus–chromium and phosphorus–carbon bonds shorten while the phosphorus-halogen bonds become elongated (Table 4) (IR stretching frequencies are given in the Supporting Information).

Including the lithium cation binding into the computational model effected a significant P–X bond lengthening while the P–W bond became shorter (Table 5; information about the energetics of type **VII** and **VII′** isomers can be found in the Supporting Information). Especially remarkable is the structure of complex **18** (type **VII** with X = Cl) which is the only example within the whole set of complexes **17**–**24** in which *the Li–Cl distance clearly exceeds the sum of covalent radii* of 2.32 Å recently set up by Pykkö and Atsumi.[47] The weak bonding of a chloride coincides with the largest sum of bond angles (not including those involving lithium) at phosphorus and, in addition, the longest phosphorus–carbon (1.890 Å) and phosphorus–tungsten bonds (2.631 Å).

Structures and Spectroscopic Properties of Tungsten Complexes of Types A-D, C*, D*. Coordination of a 12-crown-4 ether and/or diethylether ligand to the lithium atoms of isomer types **VII** and **VII′** (of the *P*-Me model system) gives rise to four principal structure types **A-D** of "solvated" complexes (Scheme 4). The computed molecular structures are shown in Figure 2, and metric parameters are listed in Table 6 (selected vibrational frequencies of the tungsten complexes as well as results on the chromium series and on structures excluding 12-crown-4 (structure types **VII** and **VII′**) can be found in the Supporting Information). The molecular structures of the contact-ion pairs **A-D** differ in the coordination numbers at phosphorus (four in type **A**,**C** or three in **B**,**D**), the coordination site of the cation (at phosphorus in **A**,**C**, at the halogen in **B**,**D**), and the binding

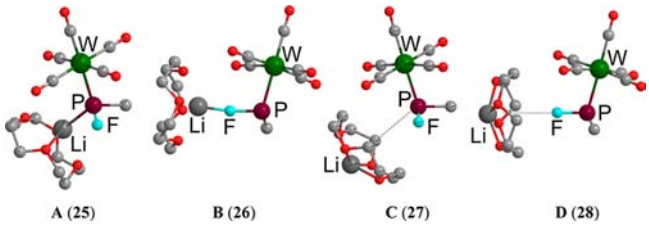

Figure 2. Reduced view (hydrogens omitted) of contact-ion pairs **A-D** of model phosphinidenoid complexes $[Li(12\text{-crown-}4)][(CO)_5W\{P(Me)F\}]$ (**25**–**28**) (VWNBP86/TZ2P SO ZORA, ADF 2007.1); a figure of structure type **C*** (the real system including microsolvation at Li) is included in the Supporting Information.

Table 5. Bond Lengths [Å] and Sum of Angles [deg] (Excluding Lithium) of Lithium/Halo-Phosphinidenoid Complexes $Li[(CO)_5W\{P(CH(SiMe_3)_2)X\}]$ (Structure Type VII: 17–20, type VII′: 21–24) at B3LYP/6-311g(d,p), LanL2DZ(W); for Comparison Pyykkö's Sum of Covalent Li-X Radii Is Included[47]

	type	X	W–P [Å]	P–X [Å]	P–Li [Å]	Li-X[a] [Å]	P–C [Å]	∑∠P [deg]
17	**VII**	F	2.554	1.895	2.382	1.751 (1.97)	1.863	316.5
18	**VII**	Cl	2.631	2.160	2.416	3.774 (2.32)	1.890	338.2
19	**VII**	Br	2.589	2.562	2.451	2.412 (2.47)	1.863	332.3
20	**VII**	I	2.525	2.939	2.388	2.576 (2.66)	1.878	334.2
21	**VII′**	F	2.644	1.911	3.142	1.720 (1.97)	1.856	310.7
22	**VII′**	Cl	2.596	2.697	3.698	2.140 (2.32)	1.841	318.0
23	**VII′**	Br	2.600	2.867	3.825	2.297 (2.47)	1.845	320.6
24	**VII′**	I	2.584	3.242	4.105	2.517 (2.66)	1.841	325.0

[a]Values in parentheses denote the sum of covalent radii as given by Pykkö and Atsumi.[47]

dx.doi.org/10.1021/ic302786v | *Inorg. Chem.* 2013, 52, 3313–3325

Table 6. Bond Lengths [Å] and Sum of Angles [deg] for Lithium/Fluoro Phosphinidenoid Complexes [Li(12-crown-4)][$(CO)_5$W{P(Me)F}] (25,26) and [Li(12-crown-4)Et_2O][$(CO)_5$W{P(R)F}] (R = Me (27,28), $CH(SiMe_3)_2$ (29)) in the Gas Phase[a]

	type	method	W−P [Å]	P−F [Å]	P−C [Å]	P−Li [Å]	Li−F [Å]	∑∠P [deg]
25	**A**	i	2.601	1.699	1.855	2.475	3.236	315.6
		ii	2.588	1.683	1.856	2.493	3.209	316.2
26	**B**	i	2.616	1.806	1.863	3.566	1.769	303.6
		ii	2.608	1.760	1.864	3.525	1.775	306.4
27	**C**	i	2.623	1.744	1.860	5.086	4.501	310.1
		ii	2.615	1.701	1.865	5.082	5.018	310.8
		i[b]	2.626	1.740	1.861	5.374	4.787	309.9
28	**D**	i	2.623	1.785	1.865	5.649	3.887	304.1
		ii	2.608	1.737	1.864	5.676	3.956	307.0
		i[b]	2.626	1.779	1.865	5.964	4.202	304.1
29[c]	**C**	ii[b]	2.637	1.704	1.887	5.471	5.679	313.6

[a]Calculations were carried out at the B3LYP/6-311g(d,p)-LanL2DZ(W) (G09, method i)) or VWNBP86/TZVP SO ZORA (ADF, method ii) level. Entries citing table footnote *b* include microsolvation at lithium. [b]= microsolvation at lithium through coordination of Et_2O. [c]= $CH(SiMe_3)_2$.

of 12-crown-4 in a "front-sided" (**A**,**B**) or "back-sided" (**C**,**D**) fashion (Figure 2).

The tungsten−phosphorus bond lengths calculated at the B3lyp/6-311g(d,p), LanL2DZ(W) level vary from 2.601 Å (**A**) to 2.623 Å (Table 6, method i; **C***,**D*** with inclusion of microsolvation at Li) in the gas phase, which is generally longer than those calculated with a scalar relativistically corrected all electron method (VWNBP86/TZVP SO ZORA, method ii).

Simulation of an ethereal solution within the SMD model produces further elongation and, again, the real system **29** possesses the largest distance (W−P 2.637 Å). In contrast, most phosphorus−fluorine (exception: **A**) and phosphorus−carbon bonds are shortened upon going from gas phase to solution. Phosphorus−fluorine bonds roughly vary from 1.7 to 1.8 Å, but the phosphorus−carbon bonds remain almost constant at 1.86 Å in all four structure types. Sums of angles at phosphorus are generally small and vary from 304° to 316°. Only structural type **B** contains a "molecular" lithium-fluoride moiety with a bond length of 1.77 Å, while in all other isomers lithium and fluorine are well separated at distances between 3.2 Å in **A** and 4.5 Å in **C**.

To mimic the real structure of complex **6a** in the crystal, we calculated the structure of [Li(12-crown-4)Et_2O][$(CO)_5$W{P-($CH(SiMe_3)_2$)F}] (**29**), modeling the ion-pair contact between the anionic phosphorus moiety and the back-sided Li(12-crown-4) cation in silico by including microsolvation at lithium by a molecule of Et_2O (based on structure type **C**; the corresponding figure showing **29** can be found in the Supporting Information). The results of the calculation (VWNBB86/TZ2P SO ZORA (ADF)) suggest a pyramidal environment at phosphorus with a P−F distance of 1.704 Å (**6a**: 1.744(9) Å), a P−W distance of 2.637 Å (**6a**: 2.580(3) Å), and a P−C distance of 1.887 Å (**6a**: 1.8402(1) Å).

To get further insight into the connections between bond distances and bond strengths, compliance constants were calculated (Figure 3).[41]

Compared with fluorophosphane H_2PF, used here as the phosphorus−fluorine single bond reference, the P−F bond compliances generally increase by 38% for the free anionic complex [$(CO)_5$W{P(Me)F}]$^-$ (**10a**), by 46% upon coordination of the Li(12-crown-4) counterion for structure type **A** (**25**), and by more than 100% for structure types **B**-**D** (**26**−**28**). This means that the P−F bond is extremely weakened in going

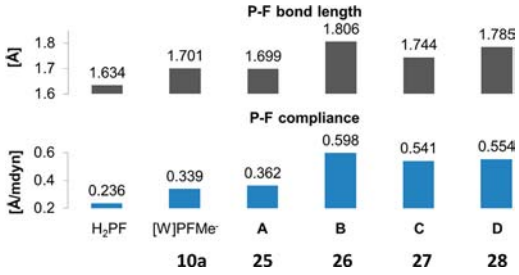

Figure 3. Comparison of P−F bond lengths and compliance constants in model phosphine H_2PF, phosphanido complex [$(CO)_5$W{P(Me)-F}]$^-$ (**10a**) and phosphinidenoid complex [Li(12-crown-4)]-[$(CO)_5$W{P(Me)F}] in structure types **A**-**D** (**25**−**28**); at B3LYP/6-311g(d,p), LanL2DZ(W).

from **10a** to **A**/**25** and **B**-**D**/**26**−**28**, and clearly reveals the destabilizing effect that is exerted by tight or loose coordination of the cationic unit. These structural and bonding features also have interesting consequences with regard to the ^1J(P,F) couplings (cf. Figure 5).

Of particular interest for this study was the change in relative energies of structural types **A**-**D** depending on the level of theoretical treatment. For the tungsten complexes the situation is as follows: in the gas phase and excluding microsolvation at lithium, structure type **B** is energetically most favored and structure types **C** and **D** are most disfavored (**25**−**28**, Figure 4).

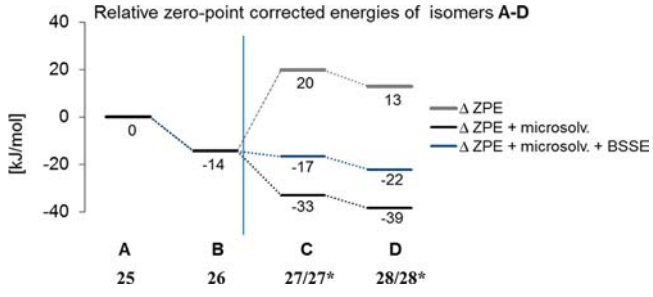

Figure 4. Relative energies (zero-point corrected energies ΔZPE and Δ*G*) in [kJ/mol] of structure types **A**-**D** and **C***, **D***, respectively, of complex [Li(12-crown-4)][$(CO)_5$W{P(Me)F}], at B3LYP/6-311g-(d,p), Lan2DZ(W) level; "microsolv." = microsolvation at lithium (Et_2O·Li), "BSSE" = basis set superposition error.

dx.doi.org/10.1021/ic302786v | *Inorg. Chem.* 2013, 52, 3313−3325

Table 7. ^{31}P NMR Chemical Shifts ($\delta(^{31}P)$), and Paramagnetic (σ^{p}) and Spin-Orbit (σ^{so}) Contributions to the Absolute Isotropic Shielding ($\sigma^{iso}(^{31}P)$) of Halophosphanido Complexes $[(CO)_5M\{P(R)X\}]^-$ (R = Me (10a−c), $CH(SiMe_3)_2$ (11−14)) at (VWNBP86/TZ2P SO ZORA, ADF 2007.1); the Experimental Values of 6a, 7a, 8, and 9 Are Given for Comparison

	M	R	X	$\delta(^{31}P)^{exp}$ [ppm]	$\delta(^{31}P)$ [ppm]	σ^{p} [ppm]	σ^{so} [ppm]
10a	W	Me	F		357	−1023	33
10b	Mo	Me	F		384	−1040	20
10c	Cr	Me	F		387	−1038	17
6a/11	W	$CH(SiMe_3)_2$	F	305.9	379	−1049	35
7a/12	W	$CH(SiMe_3)_2$	Cl	212.9	312	−989	41
8/13	W	$CH(SiMe_3)_2$	Br	242.8	361	−1040	44
9/14	W	$CH(SiMe_3)_2$	I	215.3	337	−1009	36

We then focused on **C** (**27**) and **D** (**28**) and included microsolvation by coordination of an Et_2O moiety at lithium (**C-27*** and **D-28***). Consideration of this effect together with an additional correction for basis set superposition error reverses this trend: now the energy levels of structure types **C-27*** and **D-28*** are significantly lowered on the basis of zero-point and BSSE corrected energies (Figure 4) .

^{31}P- and ^{183}W-NMR Chemical Shifts of Complexes 10a−c, 11−14, 25−29. In a preliminary study[9] we had tried to draw structural conclusions from calculated isotropic ^{31}P NMR chemical values of the Li/F phosphinidenoid complex **29** without having considered naked halophosphanido complexes **10a−c** and **11−14**, or the existence of a lithium-bound Et_2O unit. Therefore, a thorough reinvestigation was performed starting with calculations of anionic complexes **10a−c** and **11−14** which was now of particular interest as DOSY experiments had led to the conclusion that such complexes could exist as tight and/or solvent separated ion pairs.

As already described in the Introduction, the DFT-GIAO method developed by Ziegler[41b,c,43a] was used for calculations of diamagnetic (σ^{d}), paramagnetic (σ^{p}), and spin−orbit (σ^{so}) coupling contributions for the nuclei ^{31}P and ^{183}W (further details are given in the tables). The calculated ^{31}P NMR chemical shifts of model complexes **10a−c** and **11−14** of 312−379 ppm (Table 7) are generally larger than the observed ones of the real compounds **6a**, **7a**, **8**, and **9** (215−306 ppm, Table 1) but show a similar response to changes in the substituents. Thus, the chemical shifts of **10a−c** (R = Me) decrease continuously with increasing atomic number of the metal atom, whereas the ^{31}P NMR chemical shifts of **11−14** (R = $CH(SiMe_3)_2$) show no regular ordering when the halogen substituent is varied within the group: the chemical shifts decrease regularly from 379 ppm (**11**, X = F) to 361 ppm (**13**, X = Br) and 337 ppm (**14**, X = I), but the chlorine derivative **12** represents an outlier with a much lower chemical shift (312 ppm) than all other derivatives. The ^{31}P NMR chemical shifts of all halophosphanido complexes are dominated by the paramagnetic contribution (diamagnetic contributions are almost constant at σ^{d} = 958 ppm); for (neutral) complexes $[(CO)_5W(PX_3)]$ this was first reported by Kaupp.[43b] Especially noteworthy is that the smallest chemical shift was found for the chlorine derivative **12** which reproduces the irregular trend in the chemical shifts of complexes **6a**, **7a**, **8**, and **9**. Spin−orbit contributions generally increase from chromium to tungsten and, for a given metal (tungsten) from fluorine to bromine, not to iodine. The maximal spin−orbit contribution was found for X = Br amounting to 44 ppm.

In contrast, the trends in ^{183}W NMR chemical shifts for the halophosphanido complexes **10a** and **11−14** (Table 8) are perfectly regular. In going from X = fluorine to iodine the ^{183}W NMR chemical shift moves downfield. For a given halogen (X = F), the increasing steric demand of the organic substituent at phosphorus effects a downfield shift in going from R = Me (**10a**) to $CH(SiMe_3)_2$ (**11**). Diamagnetic contributions and spin−orbit contributions to ^{183}W NMR chemical shifts are almost constant at σ^{d} = 8628 ppm and σ^{so} = 2133−2147 ppm, respectively; such a relative invariance was reported earlier for other tungsten compounds by Ziegler et al.[41c] Hence, ^{183}W NMR chemical shifts of halophosphanido complexes $[(CO)_5W\{P(R)X\}]^-$ follow strictly the trends given by the paramagnetic contribution.

Table 8. ^{183}W NMR Chemical Shifts ($\delta(^{183}W)$), and Paramagnetic (σ^{p}) and Spin-Orbit (σ^{so}) Contributions to the Absolute Isotropic Shielding ($\sigma^{iso}(^{183}W)$) of Halophosphanido Complexes $[(CO)_5W\{P(R)X\}]^-$ (R = Me (**10a**), $CH(SiMe_3)_2$ (**11−14**)) at (VWNBP86/TZ2P SO ZORA, ADF 2007.1)

	M	R	X	$\delta(^{183}W)$ [ppm]	σ^{p} [ppm]	σ^{so} [ppm]
10a	W	Me	F	−3170	−4771	2135
11	W	$CH(SiMe_3)_2$	F	−3091	−4819	2133
12	W	$CH(SiMe_3)_2$	Cl	−3055	−4857	2136
13	W	$CH(SiMe_3)_2$	Br	−3029	−4889	2142
14	W	$CH(SiMe_3)_2$	I	−2997	−4926	2147

To estimate the influence of the bound Li(12-crown-4) cation on the NMR properties of fluorophosphanido complex **10a**, we then calculated appropriate chemical shifts for the Li/F phosphinidenoid complexes **25−28** and **29** (structure types **A-D**; for the Cl, Br, and I derivatives see the Supporting Information). The variation of the scalar relativistically corrected[48] DFT ^{31}P NMR chemical shifts given in Table 9 is again dominated by changes in σ^{p} whereas the diamagnetic contributions ($\sigma^{d} \approx$ 958 ppm) and spin−orbit contributions (σ^{so} = 36−40 ppm) are similar as in **11−14**;[48] Eigenvalues, span and isotropic chemical shift of the ^{31}P and ^{19}F NMR chemical shift tensors can be found in the Supporting Information. Phosphorus is most deshielded in **26** (**B**) and **28** (**D**) whereas the difference between **10a** ($\delta(^{31}P)$ = 357), **25** ($\delta(^{31}P)$ = 322), and **27** ($\delta(^{31}P)$ = 364) is small or even negligible. Going to the real system (R = $CH(SiMe_3)_2$) allowed for a discrimination between the naked anion **11** ($\delta(^{31}P)$ = 379) and structure types **C** (**29**: $\delta(^{31}P)$ = 359) and **C*** (**30**: $\delta(^{31}P)$ = 358).

The calculated ^{183}W NMR chemical shifts of the Li/F phosphinidenoid complexes **25−29** (structure types **A-D**) are almost invariant, whereby diamagnetic contributions and spin−

dx.doi.org/10.1021/ic302786v | Inorg. Chem. 2013, 52, 3313−3325

Table 9. ^{31}P NMR Chemical Shifts, $\delta(^{31}P)$, and Paramagnetic (σ^{P}) and Spin-Orbit (σ^{SO}) Contributions to the Absolute Isotropic Shielding ($\sigma^{iso}(^{31}P)$) of Lithium(12-crown-4)/Fluoro Phosphinidenoid Complexes [Li(12-crown-4)][(CO)$_5$W{P(R)F}] (Structure Types A-D, R = Me (25−28), C^R: R = CH(SiMe$_3$)$_2$ (29) and C^R*(with Et$_2$O) (30)) (cf. Figure 2), at VWNBP86/TZ2P SO ZORA, ADF 2007.1

		R	$\delta(^{31}P)$ [ppm]	σ^{P} [ppm]	σ^{so} [ppm]
25	**A**	Me	322	−993	40
26	**B**	Me	522	−1191	36
27	**C**	Me	364	−1033	37
29	**C^R**	CH(SiMe$_3$)$_2$	359	−1025	37
30	**C^R***	CH(SiMe$_3$)$_2$	358	−1026	37
28	**D**	Me	456	−1126	36

orbit couplings are almost constant at 8627 ppm and +2136 ppm, respectively (see Supporting Information). Comparison of the experimentally determined chemical shift values for **6a** ($\delta(^{31}P)$ = 306 ppm and $\delta(^{183}W)$ = −3230 ppm) with the calculated values for various bonding situations in naked halophosphanido tungsten complexes **10a**, **11**−**14**, and Li-(crown-4) coordinated complexes **25**−**29** and **30** made obvious that only the phosphorus chemical shift is indicative for the bonding, and here the paramagnetic contribution σ^{P} dominates in all cases. The values for **26** and **28** immediately reveal that even a weak F−Li interaction can be excluded for the situation in solution, as it would lead to a significant large downfield shift (**10a** → **26** or **28**); such an interaction can be rationalized in terms of a partially formed molecular LiF leaving group and, concomitantly, a terminal phosphinidene complex unit. A bonding such as in **25** should enable to detect a P−Li contact at lower temperatures, but is also contradicted by the DOSY results. Last but not least, the molecular intercalated 12-crown-4 moiety (into the P−Li contact) in **29** leads to a downfield-shift (compared to **27**). Unfortunately, additional coordination of Et$_2$O to lithium in **30** has no significant effect on the chemical shift value.

As the ^1J(P,E) coupling constants are the only other observables in the NMR spectra (besides the chemical shift), and the phosphorus−tungsten and phosphorus−fluorine bonds were mostly effected by the lithium coordination, we decided to calculate the ^1J(W,P) and ^1J(P,F) coupling constant values and to examine the correlation with the reciprocal compliance constants ("relaxed force constants" (RFC)) (Figure 5); the latter were chosen to make intrinsic bond strengths apparent.

The tungsten−phosphorus couplings for the Li/F phosphinidenoid complexes **25**−**28** have very small values (7 to 43 Hz) and although these differ numerically from the experimental values of the coupling constant magnitude of **6a** (^1J(W,P) = 71.3 Hz), the range is quite close. The calculated ^1J(P,F) values are in very good agreement with the experimental values and reveal a clear correlation with calculated PF distances and compliance constants; no such correlation was found for the PW RFCs and the ^1J(W,P) couplings. It is evident from Figure 5 that a more negative phosphorus−fluorine coupling constant is associated with a larger RFC—except for structure type **D**—and thus a stronger and shorter bond (cf. Figure 3). In turn, the smallest ^1J(P,F) values arise from F−Li contacts (short or long) which comes together with the weakest P−F bonds in **B** and **D** (= smallest RFC values). Using this correlation it can be concluded that not only the absence or presence of a cationic entity is clearly reflected by the (negative) ^1J(P,F) value but also the positioning relative to the fluorophosphanido complex unit.

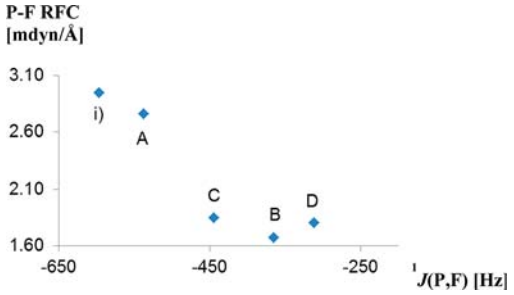

Figure 5. Correlation of P−F relaxed force constants (RFC), at B3LYP/6-311g(d,p), LanL2DZ(W), with ^1J(P,F) coupling constants, at VWNBP86/TZ2P SO ZORA, for (i) fluorophosphanido complex [(CO)$_5$W(PMeF)]$^-$ (**10a**) and phosphinidenoid complexes [Li(12-crown-4)][(CO)$_5$W{P(R)F}] (structure types **A-D**, R = Me (**25**−**28**)).

CONCLUSIONS

This first comprehensive study describes synthesis and NMR spectroscopic data of a homologue series of Li/X phosphinidenoid metal complexes (M = Cr−W; X = F−I) and, in addition, the first single-crystal X-ray structure of [Li(12-crown-4)Et$_2$O][(CO)$_5$W{P(CH(SiMe$_3$)$_2$)F}] (**6a**). The study reveals metal and halogen dependencies of NMR parameters as well as thermal stabilities of such derivatives in solution (F > Cl > Br > I). Experimental insight into the bonding in solution was obtained from DOSY experiments on the Li/F phosphinidenoid metal complexes (**6a**−**c**; M = W, Mo, Cr) and allows us to rule out that the cation and anion fragments of **6a**−**c** are part of a persistent molecular complex or tight ion pair. The X-ray structure of **6a** confirmed this bonding situation for the solid state in showing long (compared to **2a**) bond distances (P−F 1.744(9) and P−W 2.580(3) Å), while the P−C bond is affected to a lesser extent. DFT calculations provide additional insight into structures and energetics of (anionic) halophosphanido complexes [(CO)$_5$M{P(R)X}] and four contact ion pairs of Li/F phosphinidenoid model complexes [Li(12-crown-4)][(CO)$_5$M{P(R)F}] (**A**-**D**) that represent principal coordination modes of the Li(12-crown-4) cation toward fluorophosphanido complexes [(CO)$_5$M{P(R)F}]$^-$. Structure types with phosphorus "back-side" coordinated Li(12-crown-4) (**C**) and with fluorine "back-side" coordinated Li(12-crown-4) (**D**) are energetically most favored, and **C** reproduces the experimental solid state structure which is further improved in C* by coordination of Et$_2$O to lithium. The analysis of compliance constants suggests that the presence of a phosphorus lone pair weakens the P−F bond, in the fluorophosphanido complex [(CO)$_5$M{P(R)F}]$^-$, and that this weakening is further enhanced upon pairing of the anionic complex with a Li$^+$ or Li(12-crown-4)$^+$ counterion. Furthermore, a consistent interpretation of NMR properties was achieved from the DFT calculated ^{19}F, ^{31}P, and ^{183}W NMR chemical shifts. The trends in ^{31}P NMR shifts correspond with structural modifications, for example, the "naked" anionic complex experiences a significant shielding upon interaction with a back-side to phosphorus coordinated Li(12-crown-4) cation (structure type **C**) which may serve as model for contact ion pairs. In general, ^{31}P NMR chemical shifts are dominated by the paramagnetic contribution

dx.doi.org/10.1021/ic302786v | Inorg. Chem. 2013, 52, 3313−3325

which is smallest for the *P*-chloro substituted complex, and for the calculated data mirror the "abnormal" ^{31}P NMR shift of the Li/Cl phosphinidenoid complexes **7a−c**, which is reminiscent to similar findings for the Li/X carbenoid series. In addition, calculated ^{1}J(P,F) values reveal a clear correlation with calculated PF distances and relaxed force constants.

EXPERIMENTAL SECTION

General Procedures. All operations were performed in an atmosphere of deoxygenated and dried argon using standard Schlenk techniques with conventional glassware. Solvents were distilled from sodium wire/benzophenone in argon atmosphere. Melting points were determined with a Büchi apparatus Type S; the values are not corrected. NMR data of phosphane complexes **2a−c**, **3a−c**, **4**, and **5** were recorded on a Bruker Avance 300 spectrometer (^{1}H: 300.13 MHz; ^{13}C: 75.5 MHz; ^{29}Si: 59.6 MHz; ^{19}F: 282.4 MHz; ^{31}P: 121.5 MHz) at 25 °C or in case of ^{1}H, ^{13}C, and ^{29}Si NMR of **2a** at 30 °C using $CDCl_3$ as solvent and internal standard. NMR data of complexes **6a−c**, **7a−c**, **8**, and **9** were recorded on Bruker Avance 300, (^{1}H: 300.13 MHz; ^{7}Li: 116.6 MHz; ^{13}C: 75.5 MHz; ^{29}Si: 59.6 MHz; ^{19}F: 282.4 MHz; ^{31}P: 121.5 MHz), Avance 400 (^{1}H: 400.13 MHz; ^{7}Li: 155.5 MHz; ^{19}F: 376.4 MHz; ^{29}Si: 79.5 MHz; ^{31}P: 162.0 MHz; ^{183}W: 16.67 MHz) or Avance 500 spectrometers (^{19}F: 470.6 MHz) at temperatures as denoted, using [D_8]THF as solvent and internal standard; shifts are referenced to tetramethylsilane (^{1}H; ^{13}C; ^{29}Si), $CFCl_3$ (^{19}F), 85% H_3PO_4 (^{31}P) and aq. $[WO_4]^{2-}$ (^{183}W). The assignment of the ^{183}W NMR signals of complex **6a** was derived from ^{1}H,^{183}W gsHMQC spectra. Measurements of diffusion coefficients were carried out at −65 °C with a pulse sequence using a double stimulated echo for convection compensation and longitudinal eddy current delay with bipolar gradient pulses.[49] The diffusion time (Δ) was generally set to 50 ms and the gradient length (δ) to 4 ms. Diffusion coefficients *D* were determined from the data by three methods implemented in the spectrometer software, namely, a fit of $\log(I/I_0)$ of selected signals vs $-D\ q^2\ (\Delta - \delta/3)$ (here, *I* is the observed intensity, I_0 the unattenuated reference intensity, *q* the gradient strength, δ the length of the gradient, and Δ the diffusion time), DOSY, and inversion of the Laplace-Transformation using the CONTIN-Algorithm. The individual results (see Supporting Information) were found to be in agreement within the estimated error limits of approximately ±7%. Electron impact (EI, 70 eV) mass spectra were recorded on a Kratos MS 50 spectrometer (selected data given). Infrared spectra were recorded on a Thermo Nicolet 380 FT-IR (selected data given). Elemental analyses were performed using an Elementar VarioEL instrument or by the company Pascher.

General Procedure for the Synthesis of Complexes 2a−c. To a suspension of 390 mg (2.0 mmol) (for **2a,c**) or 80 mg (0.41 mmol) (for **2b**) of $AgBF_4$ in 15 mL of Et_2O a solution of chloro(organo)-phosphane complexes **3a−c** (**3a**: 1.1 g (2.0 mmol); **3b**: 185 mg (0.41 mmol); **3c**: 837 mg (2.0 mmol) in 15 mL of Et_2O) was added at −40 °C and allowed to stir overnight while warming to room temperature. The cooling bath was removed, and the reaction mixture was allowed to stir for 5 days. The solvent was removed in vacuo (0.01 mbar), the violet-gray residue was suspended in 10 mL of *n*-pentane, and the clear solution containing the product was separated with a syringe. The rest of the product was extracted two more times with 5 mL of *n*-pentane, and the solvent was then removed in vacuo (0.01 mbar) from the combined *n*-pentane solutions. The obtained grayish crystalline solids were washed twice with 1 mL of *n*-pentane until the gray color disappeared.

{[Bis(trimethylsilyl)methyl(fluoro)phosphane-κP]-pentacarbonyltungsten(0)}[9] ***(2a).*** Colorless solid, crystallized from *n*-pentane; yield: 751 mg (70%); mp 59 °C; ^{29}Si{^{1}H} NMR ($CDCl_3$): δ = 0.87 (dd, ^{2}J(P,Si) = 4.4 Hz, ^{3}J(F,Si) = 1.5 Hz, $SiMe_3$), 2.52 (dd, ^{2}J(P,Si) = 10.9 Hz, ^{3}J(F,Si) = 6.2 Hz, $SiMe_3$); all other NMR, MS, IR data were described previously in ref 9; elemental analysis (%) calculated for $C_{12}H_{20}FO_5PSi_2W$: C, 26.98; H, 3.77; found: C, 27.17; H, 3.76.

{[Bis(trimethylsilyl)methyl(fluoro)phosphane-κP]-pentacarbonylmolybdenum(0)} ***(2b).*** Colorless solid, crystallized from *n*-pentane; yield: 153.0 mg (85%); mp 52 °C; ^{1}H NMR ($CDCl_3$): δ = 0.23 (d, $^{4}J_{P,H}$ = 0.8 Hz, 9H, $SiMe_3$), 0.28 (d, $^{4}J_{H,H}$ = 1.2 Hz, 9H, $SiMe_3$), 1.40 (dd, $^{3}J_{F,H}$ = 15.4 Hz, $^{3}J_{H,H}$ = 7.4 Hz, 1H, PC*H*), 8.12 (ddd, $^{1}J_{P,H}$ = 338.2 Hz, $^{2}J_{F,H}$ = 54.0 Hz, $^{3}J_{H,H}$ = 7.4 Hz, P*H*F); ^{1}H{^{31}P} NMR ($CDCl_3$): δ = 0.23 (s, 9H, $SiMe_3$), 0.28 (d, $^{4}J_{H,H}$ = 1.4 Hz, 9H, $SiMe_3$), 1.40 (dd, $^{3}J_{F,H}$ = 15.5 Hz, $^{3}J_{H,H}$ = 7.4 Hz, 1H, PC*H*), 8.12 (dd, $^{2}J_{F,H}$ = 54.1 Hz, $^{3}J_{H,H}$ = 7.4 Hz, P*H*F); ^{13}C{^{1}H} NMR ($CDCl_3$): δ = 0.3 (d, $^{3}J_{P,C}$ = 3.6 Hz, $SiMe_3$), 2.1 (pseudo t, $^{3}J_{P,C}$+ $^{4}J_{F,C}$= 2.6 Hz, $SiMe_3$), 28.4 (dd, $^{1}J_{P,C}$ = 18.1 Hz, $^{2}J_{F,C}$ = 2.9 Hz, PCH), 204.4 (dd, $^{2}J_{P,C}$ = 10.7 Hz, $^{3}J_{F,C}$ = 2.3 Hz, CO_{cis}), 209.0 (dd, $^{2}J_{P,C}$ = 30.7 Hz, $^{3}J_{F,C}$ = 1.6 Hz CO_{trans}); ^{19}F NMR ($CDCl_3$): δ = −158.0 (d_{sat}, $^{1}J_{P,F}$ = 807.8 Hz); ^{29}Si{^{1}H} NMR ($CDCl_3$): δ = 0.08 (dd,$^{2}J_{P,Si}$ = 4.4 Hz, $^{3}J_{F,Si}$ = 1.6 Hz, $SiMe_3$), 1.85 (dd,$^{2}J_{P,Si}$ = 11.8 Hz,$^{3}J_{F,Si}$ = 2.2 Hz, $SiMe_3$); ^{31}P NMR ($CDCl_3$): δ = 187.3 (dd_{sat}, $^{1}J_{P,F}$ = 808.4 Hz, $^{1}J_{P,H}$ = 338.2 Hz); ^{31}P{^{1}H} NMR ($CDCl_3$): δ = 187.3 (d_{sat}, $^{1}J_{P,F}$ = 808.7 Hz, $^{1}J_{Mo,P}$ = 161.4 Hz); MS: *m*/*z* (%): 448 [$M^{\bullet+}$, 41], 420 [(M −CO)$^{\bullet+}$, 18], 392 [(M −2CO)$^{\bullet+}$, 40], 377 [(M −2CO −CH_3)$^{\bullet+}$, 11], 364 [(M −3CO)$^{\bullet+}$, 100], 349 [(M −3CO −CH_3)$^{\bullet+}$, 18], 336 [(M −4CO)$^{\bullet+}$, 67], 308 [(M −5CO)$^{\bullet+}$, 9], 292 [(M −5CO −CH_4)$^{\bullet+}$, 32], 276 [(M −5CO −2CH_4)$^{\bullet+}$, 13], 73 [($SiMe_3$)$^{\bullet+}$, 74]; elemental analysis (%) calculated for $C_{12}H_{20}FMoO_5PSi_2$: C, 32.29; H 4.52; found: C, 33.15; H, 4.51.

{[Bis(trimethylsilyl)methyl(fluoro)phosphane-κP]-pentacarbonylchromium(0)} ***(2c).*** Colorless solid, crystallized from *n*-pentane; yield: 602 mg (75%); mp 46 °C; ^{1}H NMR ($CDCl_3$): δ = 0.24 (s, 9H, $SiMe_3$), 0.29 (d, $^{4}J_{H,H}$ = 1.2 Hz, 9H, $SiMe_3$), 1.42 (dd, $^{3}J_{F,H}$ = 15.7 Hz, $^{3}J_{H,H}$ = 6,8 Hz, 1H, PC*H*), 8.14 (ddd, $^{1}J_{P,H}$ = 347.5 Hz, $^{2}J_{F,H}$ = 55.0 Hz, $^{3}J_{H,H}$ = 6.8 Hz, P*H*F); ^{1}H{^{31}P} NMR ($CDCl_3$): δ = 0.24 (s, 9H, $SiMe_3$), 0.29 (d, $^{4}J_{H,H}$ = 0.9 Hz, 9H, $SiMe_3$), 1.42 (dd, $^{3}J_{F,H}$ = 15.6 Hz, $^{3}J_{H,H}$ = 6.7 Hz, 1H, PC*H*), 8.14 (dd, $^{2}J_{F,H}$ = 55.0 Hz, $^{3}J_{H,H}$ = 6.7 Hz, P*H*F); ^{13}C{^{1}H} NMR ($CDCl_3$): δ = 0.0 (d, $^{3}J_{P,C}$ = 3.3 Hz, $SiMe_3$), 2.0 (pseudo t, $^{3}J_{P,C}$+ $^{4}J_{F,C}$= 2.4 Hz, $SiMe_3$), 28.2 (dd, $^{1}J_{P,C}$ = 18.1 Hz, $^{2}J_{F,C}$ = 1.9 Hz, PCH), 214.9 (dd, $^{2}J_{P,C}$ = 15.5 Hz, $^{3}J_{F,C}$ = 2.9 Hz, CO_{cis}), 219.6 (d, $^{2}J_{P,C}$ = 5.8 Hz, CO_{trans}); ^{19}F NMR ($CDCl_3$): δ = −153.7 (d_{sat}, $^{1}J_{P,F}$ = 828.0 Hz); ^{29}Si{^{1}H} NMR ($CDCl_3$): δ = 0.03 (dd,$^{2}J_{P,Si}$ = 4.9 Hz, $^{3}J_{F,Si}$ = 1.5 Hz, $SiMe_3$), 2.14 (dd,$^{2}J_{P,Si}$ = 11.3 Hz,$^{3}J_{F,Si}$ = 6.5 Hz, $SiMe_3$); ^{31}P{^{1}H} NMR ($CDCl_3$): δ = 215.3 (d, $^{1}J_{F,P}$ = 827.8 Hz; IR (KBr): $\tilde{\nu}$ = 2323 (w, ν(PH)), 2070 (m,ν(CO)), 1992 (m,ν(CO)), 1940 (vs,ν(CO)), 1258 (m), 851 (m), 651 (m) cm^{-1}; MS: *m*/*z* (%): 402 [$M^{\bullet+}$, 18], 374 [(M −CO)$^{\bullet+}$, 2], 346 [(M −2CO)$^{\bullet+}$, 1], 359 [(M −CO −CH_3)$^{\bullet+}$, 2], 331 [(M −2CO −CH_3)$^{\bullet+}$, 3], 318 [(M −3CO)$^{\bullet+}$, 7], 290 [(M −4CO)$^{\bullet+}$, 50], 262 [(M −5CO)$^{\bullet+}$, 100], 246 [M −5CO −CH_4)$^{\bullet+}$, 100], 73 [($SiMe_3$)$^{\bullet+}$, 23], 52 [(Cr)$^{\bullet+}$, 26]; elemental analysis (%) calculated for $C_{12}H_{20}FO_5PSi_2Cr$: C, 35.82; H, 5.01; found: C, 35.74; H, 5.00.

General Procedure for the Synthesis of 3a−c. To a solution of [Amino(phenyl)carbene]pentacarbonylchromium complex:[50] 9,1 mmol (2,7 g); [Amino(phenyl)carbene]pentacarbonylmolybdenum complex:[51] 10,0 mmol (3.4 g); [Amino(phenyl)carbene]-pentacarbonyltungsten complex:[50b] 9,8 mmol (4,2 g)) and [bis-(trimethylsilyl)methylene]chlorophosphane[52] in 100 mL of diethylether 40 mL of triethylamine (excess) was added. Immediate precipitation of colorless triethylammonium chloride was observed. After 24 h of stirring the solvent and the excess of triethylamine were removed in vacuo (0.01 mbar), the residue was suspended in 100 mL of toluene and heated 3 h (**3a,c**) or 2 h (**3b**) at 75 °C. Then the solvents were removed in vacuo, and the black-brown residue was adsorbed on silica gel (dissolved in ca. 10 mL CH_2Cl_2 and mixed with 5 spoons of silica gel). The product was purified by column chromatography on SiO_2 (−20 °C, petroleum ether). A yellow crystalline solid was obtained after removing the solvents and, if necessary, washing the oily residue with *n*-pentane at −30 °C.

{[Bis(trimethylsilyl)methyl(chloro)phosphane-κP]-pentacarbonyltungsten(0)}[18] ***(3a).*** Yellow solid, crystallized from *n*-pentane; yield: 4.1 g (76%); mp 64 °C; all other NMR, MS, IR data were described previously in ref 18.

{[Bis(trimethylsilyl)methyl(chloro)phosphane-κP]-pentacarbonylmolybdenum(0)} ***(3b).*** Yellow solid, crystallized from

dx.doi.org/10.1021/ic302786v | *Inorg. Chem.* 2013, 52, 3313−3325

n-pentane; yield: 253.3 mg (10.1%); mp 55 °C; ^{1}H NMR ($CDCl_3$): δ = 0.27 (s, 9H, $SiMe_3$), 0.35 (s, 9H, $SiMe_3$), 0.92 (dd, $^2J_{P,H}$ = 8.9 Hz, $^3J_{H,H}$ = 1.04 Hz, 1H, PC*H*), 7.55 (dd, $^1J_{P,H}$ = 331.9 Hz, $^3J_{H,H}$ = 1.0 Hz, 1H, P*H*Cl); ^{13}C{^{1}H} NMR ($CDCl_3$): δ = 0.8 (d, $^3J_{P,C}$ = 2.9 Hz, $SiMe_3$), 2.1 (d, $^3J_{P,C}$ = 4.2 Hz, $SiMe_3$), 24.4 (d, $^1J_{P,C}$ = 9.7 Hz, PCH), 204.3 (d, $^2J_{P,C}$ = 9.4 Hz, CO_{cis}), 209.1 (d, $^2J_{P,C}$ = 33.3 Hz, CO_{trans}); ^{29}Si NMR ($CDCl_3$): δ = 2.89 (d,$^2J_{P,Si}$ = 4.7 Hz, $SiMe_3$), 3.57 (d,$^2J_{P,Si}$ = 9.5 Hz, $SiMe_3$); ^{31}P NMR ($CDCl_3$): δ = 88.9 (dd, $^1J_{P,H}$ = 331.9 Hz, $^2J_{P,H}$ = 7.6 Hz); ^{31}P{^{1}H} NMR ($CDCl_3$): δ = 88.9 (s); IR (KBr): $\tilde{\nu}$ = 2355 (vw, ν(PH)), 2080 (w, ν(CO)), 2002 (m, ν(CO)), 1954 (s, ν(CO)), 1933 (s, ν(CO)) cm^{-1}; MS: *m*/*z* (%): 464 [M$^{\bullet+}$, 12], 408 [(M −2CO)$^{\bullet+}$, 12], 380 [(M −3CO)$^{\bullet+}$, 47], 324 [(M −5CO)$^{\bullet+}$, 39], 308 [(M −5CO −CH_4) $^{\bullet+}$, 22], 73 [($SiMe_3$)$^{\bullet+}$, 100].

*{[Bis(trimethylsilyl)methyl(chloro)phosphane-κP]pentacarbonylchromium(0)} (**3c**).* Yellow solid, crystallized from *n*-pentane; yield: 1.67 g (45%); mp 61 °C; ^{1}H NMR ($CDCl_3$): δ = 0.28 (s, 9H, $SiMe_3$), 0.36 (s, 9H, $SiMe_3$), 0.93 (d, $^2J_{P,H}$ = 7.7 Hz, 1H, PC*H*), 7.58 (d, $^1J_{P,H}$ = 341.4 Hz, 1H, P*H*Cl); ^{1}H {^{31}P} NMR ($CDCl_3$): δ = 0.28 (s, 9H, $SiMe_3$), 0.36 (s, 9H, $SiMe_3$), 0.93 (s, 1H, PC*H*), 7.58 (s, 1H, P*H*Cl); ^{13}C{^{1}H} NMR ($CDCl_3$): δ = 0.0 (d, $^3J_{P,C}$ = 2.6 Hz, $SiMe_3$), 2.1 (d, $^3J_{P,C}$ = 3.9 Hz, $SiMe_3$), 24.8 (d, $^1J_{P,C}$ = 8.7 Hz, PCH), 214.9 (d, $^2J_{P,C}$ = 13.9 Hz, CO_{cis}), 219.8 (d, $^2J_{P,C}$ = 5.5 Hz, CO_{trans}); ^{29}Si NMR ($CDCl_3$): δ = 2.9 (d,$^2J_{P,Si}$ = 5.3 Hz, $SiMe_3$), 3.23 (d,$^2J_{P,Si}$ = 10.2 Hz, $SiMe_3$); ^{31}P NMR ($CDCl_3$): δ = 123.5 (dd, $^1J_{P,H}$ = 342.1 Hz, $^1J_{P,H}$ = 7.6 Hz); ^{31}P{^{1}H} NMR ($CDCl_3$): δ = 123.5 (s); IR (KBr): $\tilde{\nu}$ = 2355 (vw, ν(PH)), 2073 (m, ν(CO)), 1999 (s, ν(CO)), 1927 (vs, ν(CO)) cm^{-1}; MS: *m*/*z* (%): 418 [M$^{\bullet+}$, 18], 334 [(M −3CO)$^{\bullet+}$, 9], 306 [(M −4CO)$^{\bullet+}$, 33], 278 [(M −5CO)$^{\bullet+}$, 76], 262 [(M −5CO −CH_4)$^{\bullet+}$, 100], 246 [(M −5CO −2CH_4)$^{\bullet+}$, 5], 73 [($SiMe_3$)$^{\bullet+}$, 49], 52 [(Cr)$^{\bullet+}$, 25]; elemental analysis (%) calculated for $C_{12}H_{20}ClCrO_5PSi_2$: C, 34.41; H, 4.81; found: C, 34.42; H, 4.92.

{[Bis(trimethylsilyl)methyl(bromo)phosphane-κP]pentacarbonyltungsten(0)}[19] *(**4**).* A solution of 1.0 mmol (618 mg) of **1a** and 1.0 mmol (206 mg) of triethylammonium bromide in 10 mL of toluene was heated 3 h at 75 °C. The solvent was then removed in vacuo, and the obtained raw product was purified by low temperature column chromatography (−20 °C; SiO_2) using petroleum ether. After removing the solvent and drying in vacuo (0.01 mbar) yellow crystals were obtained. Yield: 209 mg (0.28 mmol, 35%); mp 71 °C (decomp.); all other NMR, MS, IR data were described previously in ref 19; elemental analysis (%) calculated for $C_{12}H_{20}BrO_5PSi_2W$: C, 24.22; H, 3.39; found.: C, 24.52; H, 3.67.

{[Bis(trimethylsilyl)methyl(iodo)phosphane-κP]pentacarbonyltungsten(0)}[20] *(**5**).* To a cooled solution (ice bath) of 10 mmol (2.25 g) of [bis(trimethylsilyl)methylene]chlorophosphane in 100 mL of *n*-pentane about 15 mmol (ca. 3.0 g) of iodotrimethylsilane was added slowly with a syringe. The reaction mixture was allowed to stir 2 h in an ice-bath. After the solvent was removed in vacuo an orange oil was obtained as raw product. In the next step a solution of about 9.8 mmol (4.2 g) pentacarbonyl[amino(phenyl)carbene]tungsten(0) in 100 mL of diethylether was added to the orange oil obtained beforehand and 40 mL of triethylamine was added to this mixture. After 19 h of stirring diethyl ether and triethylamine were removed in vacuo, the residue was dissolved in 100 mL of toluene and heated 3 h at 75 °C. The solvent was removed, and the product was purified by low temperature column chromatography (−20 °C; SiO_2) using petroleum ether as eluent. Petroleum ether was removed from the first yellow fraction, and the obtained yellow oil was washed with about 2 mL of *n*-pentane at −100 °C. The yellow oil was dried in vacuo until a yellow-orange solid formed, which was then stored (light protected under 12 °C). Yield: 233 mg (0.28 mmol, 36%); mp 64 °C (decomp.); all other NMR, MS, IR data were described previously in ref 20; elemental analysis (%) calculated for $C_{12}H_{20}IO_5PSi_2W$: C, 22.44; H, 3.14; found.: C, 22.86; H, 3.29.

General Procedure for the Generation of 6a−c, 7a−c, 8, and 9 (for NMR Characterization). A 0.11 mmol portion of an LDA solution, freshly prepared in a "finger-Schlenk" tube with 0.3 mL of [D_8]THF was transferred into a NMR tube using a double-ended cannula at room temperature and cooled afterward to −80 °C. A cooled (ca. 0 °C) solution of 0.1 mmol halogenophosphane complex **2a−c**, **3a−c**, **4a** or **5a** and 0.1 mmol 12-crown-4 in 0.3 mL of [D_8]THF, respectively, was then added slowly via a double-ended cannula to the LDA solution. In case of the fluorine derivative the color changed from colorless to yellow. The NMR tube was carried while cooling (between −80 and −100 °C) to the NMR spectrometer (precooled), and was shaken shortly and strongly before the measurement.

[Lithium(12-crown-4)][bis(trimethylsilyl)methyl-fluorophosphanido-κP]pentacarbonyl-tungsten(0)[9] *(**6a**).* ^{7}Li NMR (−70 °C): δ = 0.47; ^{31}P{^{1}H} NMR (−70 °C): δ = 305.9 (d_{sat}, ^1J(P,F) = 614.6 Hz, ^1J(W,P) = 71.3 Hz); ^{1}H,^{183}W-gsHMQC (−60 °C): δ(^{183}W) = −3240; ^{1}H,^{183}W-gsHMQC (−10 °C): δ (^{183}W) = −3230; all other NMR data were described in ref 9.

*[Lithium(12-crown-4)][bis(trimethylsilyl)methyl-fluorophosphanido-κP]pentacarbonyl-molybdenum(0) (**6b**).* ^{1}H NMR (−70 °C): δ = 0.00 (br s, 9H, $SiMe_3$), 0.11 (br s, 9H, $SiMe_3$), 2.91 (br s, 1H, PC*H*), 3.79 (br s, 16H, 12-crown-4); ^{1}H NMR (25 °C): δ = 0.03 (d, $^4J_{P,H}$ = 1.6 Hz, 9H, $SiMe_3$), 0.14 (d, $^4J_{P,H}$ = 1.4 Hz, 9H, $SiMe_3$), 2.90 (d, $^2J_{P,H}$ = 3.1 Hz, 1H, PC*H*), 3.80 (br s, 16H, 12-crown-4); ^{1}H{^{31}P} NMR (25 °C): δ = 0.03 (s, 9H, $SiMe_3$), 0.14 (s, 9H, $SiMe_3$), 2.90 (s, 1H, PC*H*), 3.80 (br s, 16H, 12-crown-4); ^{7}Li NMR (−60 °C): δ = −1.06; ^{13}C{^{1}H}-NMR (−70 °C): δ = 0.6 (d, $^3J_{P,C}$ = 10.0 Hz, $SiMe_3$), 3.2 (br s, $SiMe_3$), 30.0 (dd, $^1J_{P,C}$ = 82.3 Hz, $^2J_{F,C}$ ≈ 12 Hz, PCH), 66.9 m. shoulder (br s, 12-crown-4), 214.3 (d, $J_{P,C}$ = 3.9 Hz, CO_{cis}), 220.7 (d, $^2J_{P,C}$ = 12.5 Hz, CO_{trans}); ^{13}C{^{1}H}-NMR (25 °C): δ = 0.9 (d, $^3J_{P,C}$ = 11.6 Hz, $SiMe_3$), 3.4 (dd, $^3J_{P,C}$ = 3.2 Hz, $^4J_{F,C}$ = 1.6 Hz, $SiMe_3$), 30.4 (dd, $^1J_{P,C}$ = 82.1 Hz, $^2J_{F,C}$ = 14.5 Hz, PCH), 68.9 (br s, 12-crown-4), 214.4 (dd, $^2J_{P,C}$ = 4.8 Hz, $^3J_{F,C}$ = 2.3 Hz, CO_{cis}), 220.7 (d, $^2J_{P,C}$ = 12.9 Hz, CO_{trans}); ^{19}F-NMR (−60 °C, $CFCl_3$): δ = −231.3 (d, $^1J_{P,F}$ = 605.5 Hz); ^{29}Si NMR (−70 °C): δ = −2.70 (d, $^2J_{P,Si}$ = 14.7 Hz, $SiMe_3$); ^{29}Si NMR (25 °C): δ = −1.92 (d, $^2J_{P,Si}$ = 16.4 Hz, $SiMe_3$); ^{31}P{^{1}H} NMR (25 °C): δ = 343.9 (d, $^1J_{P,F}$ = 605.3 Hz).

*[Lithium(12-crown-4)][bis(trimethylsilyl)methyl-fluorophosphanido-κP]pentacarbonyl-chromium(0) (**6c**).* ^{1}H NMR (−80 °C): δ = 0.00 (br s, 9H, $SiMe_3$), 0.11 (br s, 9H, $SiMe_3$), 2.66 (br s, 1H, PC*H*), 3.74 (br s, 16H, 12-crown-4); ^{1}H NMR (25 °C): δ = −0.03 (d, $^4J_{P,H}$ = 1.4 Hz, 9H, $SiMe_3$), 0.14 (d, $^4J_{P,H}$ = 1.5 Hz, 9H, $SiMe_3$), 2.66 (s_{sat}, $^2J_{Si,H}$ = 8.0 Hz, 1H, PC*H*), 3.78 (s, 16H, 12-crown-4); ^{7}Li NMR (−60 °C): δ = −0.95; ^{13}C{^{1}H}-NMR (−80 °C): δ = 1.0 (br s_{sat}, $^1J_{P,Si}$ = 74.4 Hz, $SiMe_3$), 2.8 (br s_{sat}, $^1J_{P,Si}$ = 48.8 Hz, $SiMe_3$), 29.2 (dd, ^1J(P,C) = 85.3 Hz, ^2J(F,C) = 12.4 Hz, PCH), 66.1 (br s, 12-crown-4), 224.9 (br s, CO_{cis}), 230.7 (s, CO_{trans}); ^{13}C{^{1}H}-NMR (25 °C): δ = 1.0 (d, $^3J_{P,C}$ = 11.0 Hz, $SiMe_3$), 3.5 (dd, $^3J_{P,C}$ = 3.2 Hz, $^4J_{F,C}$ = 1.3 Hz, $SiMe_3$), 30.2 (dd, $^1J_{P,C}$ = 86.0 Hz, $^2J_{F,C}$ = 14.2 Hz, PCH), 68.9 (s, 12-crown-4), 225.7 (dd, $^2J_{P,C}$ = 6.1 Hz, $^3J_{F,C}$ = 2.3 Hz, CO_{cis}), 231.4 (s, CO_{trans}); ^{19}F-NMR (−80 °C): δ = −220.6 (d, $^1J_{P,F}$ = 664.0 Hz); ^{31}P{^{1}H}-NMR (−80 °C): δ = 345.8 (d_{sat}, $^1J_{P,F}$ = 662.5 Hz); ^{31}P{^{1}H}-NMR (25 °C): δ = 353.0 (d_{sat}, $^1J_{P,F}$ = 665.0 Hz, $^2J_{P,Si}$ = 35.0 Hz).

*[Lithium(12-crown-4)][bis(trimethylsilyl)methyl-chlorophosphanido-κP]pentacarbonyl-tungsten(0) (**7a**).* ^{1}H NMR (−70 °C): δ = 0.07 (s, 9H, $SiMe_3$), 0.16 (s, 9H, $SiMe_3$), 2.28 (br s, 1H, PC*H*), 3.74 (s, 16H, 12-crown-4); ^{13}C{^{1}H}-NMR (−70 °C): δ = 0.1 (d, $^3J_{P,C}$ = 12.4 Hz, $SiMe_3$), 3.3 (s, $SiMe_3$), 26.0 (d, $^1J_{P,C}$ = 87.4 Hz, PCH), 66.8 (br s, 12-crown-4), 204.9 (d_{sat}, $^1J_{W,C}$ = 128.4 Hz, $^2J_{P,C}$ = 4.5 Hz, CO_{cis}), 208.9 (d, $^2J_{P,C}$ = 13.9 Hz, CO_{trans}); ^{29}Si NMR (−70 °C): δ = −0.37 (s, $SiMe_3$); ^{31}P{^{1}H}-NMR (−70 °C): δ = 212.9 (br s_{sat}, ^1J(W,P) = 67.4 Hz).

*[Lithium(12-crown-4)][bis(trimethylsilyl)methyl-chlorophosphanido-κP]pentacarbonyl-molybdenum(0) (**7b**).* ^{1}H NMR (−70 °C): δ = 0.09 (s, 9H, $SiMe_3$), 0.19 (s, 9H, $SiMe_3$), 2.18 (br s, 1H, PC*H*), 3.80 (s, 16H, 12-crown-4); ^{13}C{^{1}H}-NMR (−70 °C): δ = 0.9 (d, $^3J_{P,C}$ = 12.3 Hz, $SiMe_3$), 4.1 (s, $SiMe_3$), 26.1 (d, $^1J_{P,C}$ = 89.2 Hz, PCH), 66.9 (s, 12-crown-4), 212.6 (br s, CO_{cis}), 218.8 (d, $^2J_{P,C}$ = 14.5 Hz, CO_{trans}); ^{29}Si NMR (−70 °C): δ = −0.73 (s, $SiMe_3$); ^{31}P{^{1}H}-NMR (−70 °C): δ = 245.2 (br s).

*[Lithium(12-crown-4)][bis(trimethylsilyl)methyl-chlorophosphanido-κP]pentacarbonyl-chromium(0) (**7c**).* ^{1}H NMR (−70 °C): δ = 0.09 (s, 9H, $SiMe_3$), 0.19 (s, 9H, $SiMe_3$), 1.97 (br s, 1H, PC*H*), 3.72 (s, 16H, 12-crown-4); ^{13}C{^{1}H}-NMR (−70 °C): δ = 1.0 (d, $^3J_{P,C}$ = 11.6 Hz, $SiMe_3$), 4.3 (s, $SiMe_3$), 26.1 (d, $^1J_{P,C}$ = 97.2 Hz, PCH), 66.8

dx.doi.org/10.1021/ic302786v | *Inorg. Chem.* 2013, 52, 3313−3325

(br s, 12- crown-4), 223.9 (d, $^2J_{P,C}$ = 2.9 Hz, CO_{cis}), 229.6 (s, CO_{trans}); ^{29}Si NMR (−70 °C): δ = −0.53 (s, $SiMe_3$); ^{31}P{^{1}H}-NMR (−70 °C): δ = 274.7 (s).

*[Lithium(12-crown-4)][bis(trimethylsilyl)methyl-bromophosphanido-κP]pentacarbonyl-tungsten(0) (**8**).* ^{1}H NMR (−70 °C): δ = 0.12 (s, 9H, $SiMe_3$), 0.22 (s, 9H, $SiMe_3$), 2.13 (br s, 1H, PC*H*), 3.68 (s, 16H, 12-crown-4); ^{31}P{^{1}H} NMR (CD_2Cl_2): δ = 242.8 (br s_{sat}, ^1J(W,P) = 61.0 Hz).

*[Lithium(12-crown-4)][bis(trimethylsilyl)methyl-iodophosphanido-κP]pentacarbonyl-tungsten(0) (**9**).* ^{1}H NMR (CD_2Cl_2): δ = 0.13 (s, 9H, $SiMe_3$), 0.25 (s, 9H, $SiMe_3$), 1.49 (br s, 1H, PC*H*), 3.83 (s, 16H, 12-crown-4); ^{31}P{^{1}H} NMR (CD_2Cl_2): δ = 215.3 (br s_{sat}, ^1J(W,P) = 54.5 Hz).

Synthesis and Isolation of Li/F Phosphinidenoid Complex 6a.[9] A 0.22 mmol portion of lithium diisopropylamide (freshly prepared with 0.14 mL (0.22 mmol) of a 1.6 M *n*-buthyllithium solution and 32 μL (0.22 mmol) of diisopropylamine) was dissolved in 3 mL of diethylether and cooled to −80 °C. A cooled (0 °C) solution of 107 mg (0.2 mmol) of **2a** and 34 μL (0.2 mmol) of 12-crown-4 in 3 mL of diethylether was then added to the LDA solution via double-ended cannula. A rapid color change from colorless to citreous yellow was observed. The reaction mixture was allowed to stir with temperature slowly increasing to about −50 °C. Afterward the reaction mixture was kept for about 1 h between −50 °C and −20 °C while constant stirring until a citreous yellow solid precipitated. Then stirring was stopped, and the orange solution was syringed from yellow solid with a thin needle at about 0 °C. The residue was then washed twice with 2 mL respectively cooled (ca. 0 °C) of diethylether and dried in vacuo at around 0 °C. The obtained citreous yellow, an extremely air-sensitive powder, was always prepared for further investigations under an atmosphere of dry argon.

Yield: 110 mg (77%); mp determination: inside a drybox a powder diffractometry capillary was filled with **6a** and sealed. A color change from citreous yellow to ochre-orange occurred above 30 °C and melting/decomposition at 84 °C; NMR measurements: the powder was dissolved in 0.7 mL of [D_8]THF and transferred with a double-ended cannula into an airtight Young NMR tube. The NMR spectra show the absence of formed diisopropylamine, but a mixture of **6a** and **2a**, the latter most probably formed because of partial hydrolysis, so that the amount of 12-crown-4 contained in compound **6a** could not be determined exactly by integration; IR data were described in ref 9. MS: *m*/*z* (%):886 [$M^{\bullet+}$ -(12-crown-4)-Li, 12], 772 [$M^{\bullet+}$ -(12-crown-4)-LiH -4CO, 28], 716 [$(M^{\bullet+}$, 5], 688 [$(M\text{-}CO)^{\bullet+}$, 10], 632 [$(M\text{-}3CO)^{\bullet+}$, 5], 604 [$(M\text{-}4CO)^{\bullet+}$, 12], 532 [(M-LiH -(12-crown-4)$^{\bullet+}$, 60], 504 [(M-LiH-(12-crown-4)-CO)$^{\bullet+}$, 36], 476 [(M-LiH-(12-crown-4)-2CO)$^{\bullet+}$, 80], 446 [(M-LiH-(12-crown-4)-2COC_2H_6)$^{\bullet+}$, 92], 418 [(M-LiH-(12-crown-4)-3CO-C_2H_6)$^{\bullet+}$, 12], 390 [(M-LiH-(12-crown-4)-4CO-C_2H_6)$^{\bullet+}$, 100]; elemental analysis (%) calculated for [Li(12-crown-4)][$(CO)_5WP(CH(SiMe_3)_2)F$]: C, 33.53; H, 4.92; calculated for [$Li(12\text{-crown-4})_2$][$(CO)_5WP(CH(SiMe_3)_2)F$]: C, 37.68; H, 5.76; calculated for [Li(12-crown-4)(Et_2O)][$(OC)_5WP(CH(SiMe_3)_2)F$]: C, 36.46; H, 5.74; found.: C, 37.45; H, 5.55.

Single-Crystal X-ray Analysis of 2a. X-ray crystallographic analysis of complex **2a** was recorded on a Nonius KappaCCD; $C_{12}H_{20}FO_5PSi_2W$; crystal size 0.23 × 0.16 × 0.09 mm^3, M = 534.28, monoclinic, $P21/n$, a = 12.1917(3) Å, b = 13.7965(3) Å, c = 13.1040(2) Å, α = 90°, β = 116.983(1)°, γ = 90°, V = 1964.19(7) Å^3, Z = 4, d_{calc} = 1.807 Mg/m^3, μ = 6.108 mm^{-1}, T = 110(2) K, $2\theta_{max}$ = 54.96°, collected (unique) reflections =36635 (4500), R_{int} = 0.0595, absorption correction: semiempirical from equivalents (max./min. Transmission = 0.6094/0.3340), refinement method: full-matrix least-squares on F^2, 215 refined parameters, R values [$I > 2\sigma(I)$]: R_1 = 0.0290, wR_2 = 0.0673. R values [all data]: R_1 = 0.0341, wR_2 = 0.0691, Min./max. difference electron density: −2.432/1.688 e Å^{-3}.

Single-Crystal X-ray Analysis of 6a. X-ray crystallographic analysis of complex **6a** was recorded on a STOE IPDS 2T; $C_{24}H_{45}FLiO_{10}PSi_2W$; crystal size 0.06 × 0.04 × 0.01 mm^3, M = 790.54, monoclinic, $P21/n$, a = 9.6547(5) Å, b = 17.6170(10) Å, c = 21.8186(12) Å, α = 90°, β = 93.024(4)°, γ = 90°, V = 3705.9(4) Å^3, Z = 4, d_{calc} = 1.417 Mg/m^3, μ = 3.272 mm^{-1}, T = 123(2) K, $2\theta_{max}$ = 54°, collected (unique) reflections = 24149 (8075), R_{int} = 0.1073, absorption correction: semiempirical from equivalents (max./min. Transmission = 0.6795/0.3919), refinement method: full-matrix least-squares on F^2, 369 refined parameters, R values [$I > 2\sigma(I)$]: R_1 = 0.0731, wR_2 = 0.1515. R values [all data]: R_1 = 0.1650, wR_2 = 0.1830, Min./max. difference electron density: −1.084/0.989 e Å^{-3}.

Crystallographic data for the structures reported in this paper have been deposited with the Cambridge Crystallographic Data Centre as supplementary publication no. CCDC-888696 (**2a**) and CCDC-888695 (**6a**). Copies of the data can be obtained free of charge on application to Cambridge Crystallographic Data Centre, 12 Union Road, Cambridge CB21EZ, U.K. (fax (+44)1223-336-033) or via e-mail (deposit@ccdc.cam.ac.uk) or from the url (www.ccdc.cam.ac.uk/data_request/cif).

■ ASSOCIATED CONTENT

Ⓢ Supporting Information

Table S1, temperature dependent NMR spectra of **6a**; Table S2, DOSY NMR results for **6a−c**, **2a**, and **12-crown-4**; Table S3, stretching frequencies of halophosphanido complexes **10a−c**, **11−14**; Table S4, stretching frequencies of halophosphanido complexes **10c**, **15**, **16**; Figure S1, structure of phosphanido complex **1** and Li/F phosphinidenoid complexes **2**, **3**; Table S5, bond lengths and stretching frequencies complex **1** and two isomers **2** and **3**; Figure S2, zero point corrected energies of complexes **4a−d** and **5a−d**; Figure S3, structure of Li/F phosphinidenoid complexes **4a** and **5a**; Table S6, stretching frequencies of **6−9** (gas phase and solution); Figure S4, structure of [$Li(12\text{-crown-4})Et_2O$][$(CO)_5W\{P(CH(SiMe_3)_2)F\}$] (**30**); Table S7, stretching frequencies of Li/F phosphinidenoid complexes **25−28** (gas phase); Table S8, compliance constants, $\delta(^{31}P)$, $\delta(^{183}W)$, ^1J(W,P), ^1J(P,F) of complexes **10−15**; Table S9, ^{183}W NMR chemical shifts, σ^p and σ^{SO} contributions of complexes **25−29**. This material is available free of charge via the Internet at http://pubs.acs.org.

■ AUTHOR INFORMATION

Corresponding Author

*Fax: +49 228 739616. Phone: +49 228 735345. E-mail: r.streubel@uni-bonn.de.

Notes

The authors declare no competing financial interest.

‖D.G.: E-mail: gudat@iac.uni-stuttgart.de.

■ ACKNOWLEDGMENTS

We thank the Deutsche Forschungsgemeinschaft (STR 411/26-1) and the Cost action cm0802 "PhoSciNet" for financial support. G.S. thanks Prof. Dr. A. C. Filippou for support.

■ DEDICATION

This work is dedicated to Prof. D. Seebach on the occasion of his 75th birthday

■ REFERENCES

(1) (a) Ziegler, K.; Gellert, H. G. *Liebigs Ann. Chem.* **1950**, *567*, 185−195. (b) Schöllkopf, U.; Eisert, M. *Angew. Chem.* **1960**, *72*, 349−350. (c) Hoberg, H. *Liebigs Ann. Chem.* **1962**, *656*, 1−14. (d) Schöllkopf, U.; Eisert, M. *Liebigs Ann. Chem.* **1963**, *664*, 76. (e) Closs, G. L.; Moss, R. A. *J. Am. Chem. Soc.* **1964**, *86*, 4042−4053. (f) Kirmse, W. *Angew. Chem., Int. Ed. Engl.* **1965**, *4*, 1−10. (g) Koebrich, G. *Angew. Chem., Int. Ed. Engl.* **1967**, *6*, 41−52. (h) Harder, S.; Boersma, J.; Brandsma, L.; Kanters, J. A.; Bauer, W.; Pi, R.; von Ragué Schleyer, P.; Schöllhorn, H.; Thewalt, U. *Organometallics* **1989**, *8*, 1688−1696. (i) Boche, G.; Opel, A.; Marsch, M.; Harms, K.; Haller, F.; Lohrenz, J. C. W.;

Thuemmler, C.; Koch, W. *Chem. Ber.* **1992**, *125*, 2265−2273. (j) Boche, G.; Bosold, F.; Lohrenz, J. C. W.; Opel, A.; Zulauf, P. *Chem. Ber.* **1993**, *126*, 1873−1885.

(2) Reviews: (a) Müller, A.; Marsch, M.; Harms, K.; Lohrenz, J. C. W.; Boche, G. *Angew. Chem.* **1996**, *108*, 1639−1640; *Angew. Chem., Int. Ed. Engl.* **1996**, *35*, 1518−1520. (b) Braun, M. *Angew. Chem., Int. Ed.* **1998**, *37*, 430−451. (c) Boche, G.; Lohrenz, J. C. W. *Chem. Rev.* **2001**, *101*, 697−756.

(3) (a) Atwell, W. H.; Weyenberg, D. R. *Angew. Chem.* **1969**, *81*, 485−493; *Angew. Chem., Int. Ed. Engl.* **1969**, *8*, 469−477. (b) Tamao, K.; Kawashi, A. *Angew. Chem.* **1995**, *107*, 886−888; *Angew. Chem., Int. Ed. Engl.* **1995**, *34*, 818−820.

(4) (a) Tamao, K.; Kawachi, A. *Organometallics* **1995**, *14*, 3108−3111. (b) Tamao, K.; Kawashi, A.; Asahara, M.; Toshimitsu, A. *Pure Appl. Chem.* **1999**, *71*, 393−400. (c) Lee, M. E.; Cho, H. M.; Lim, Y. M.; Choi, J. K.; Park, C. H.; Jeong, S. E.; Lee, U. *Chem.—Eur. J.* **2004**, *10*, 377−381. (d) Likhar, P. P.; Zirngast, M.; Baumgartner, J.; Marschner, C. *Chem. Commun.* **2004**, 1764−1765. (e) Antolini, F.; Gehrhus, B.; Hitchcock, P. B.; Lappert, M. F. *Chem. Commun.* **2005**, 5112−5114. (f) Flock, M.; Marschner, C. *Chem.—Eur. J.* **2005**, *11*, 4635−4642. (g) Weidenbruch, M. *Angew. Chem.* **2006**, *118*, 4347−4348; *Angew. Chem., Int. Ed.* **2006**, *45*, 4241−4242. (h) Zirngast, M.; Baumgartner, J.; Marschner, C. *Eur. J. Inorg. Chem.* **2008**, 1078−1087.

(5) Molev, G.; Bravo-Zhivotovskii, D.; Karni, M.; Tumanskii, B.; Botoshansky, M.; Apeloig, Y. *J. Am. Chem. Soc.* **2006**, *128*, 2784−2785.

(6) (a) Yoshifuji, M.; Shima, I.; Inamoto, N.; Hirotsu, K.; Higuchi, T. J. *J. Am. Chem. Soc.* **1981**, *103*, 4587−4589. (b) Yoshifuji, M.; Sato, T.; Inamoto, N. *Chem. Lett.* **1988**, 1735−1738. (c) Couret, C.; Escudie, J.; Satge, J. *Tetrahedron Lett.* **1982**, *23*, 4941−4942.

(7) (a) Mathey, F.; Tran Huy, N. H.; Marinetti, A. *Helv. Chim. Acta* **2001**, *84*, 2938−2957. (b) Lammertsma, K. *Top. Curr. Chem.* **2003**, *229*, 95−119. (c) Aktas, H.; Slootweg, C. J.; Lammertsma, K. *Angew. Chem., Int. Ed.* **2010**, *49*, 2102−2113.

(8) (a) Li, X.; Weissman, S. I.; Lin, T.-S.; Gaspar, P. P.; Cowley, A. H.; Smirnov, A. I. *J. Am. Chem. Soc.* **1994**, *116*, 7899−7900. (b) Bucher, G.; M. Borst, L. G.; Ehlers, A. W.; Lammertsma, K.; Ceola, S.; Huber, M.; Grote, D.; Sander, W. *Angew. Chem., Int. Ed.* **2005**, *44*, 3289−3293. (c) Niecke, E.; Streubel, R.; Nieger, M.; Stalke, D. *Angew. Chem., Int. Ed. Engl.* **1989**, *28*, 1673−1674. (d) Shah, S.; Protasiewicz, J. D. *Chem. Commun.* **1998**, 1585−1586. (e) Shah, S.; Simpson, M. C.; Smith, R. C.; Protasiewicz, J. D. *J. Am. Chem. Soc.* **2001**, *123*, 6925−6926. (f) Kilgore, U.; Fan, H.; Pink, M.; Urnezius, E.; Protasiewicz, J. D.; Mindiola, D. J. *Chem. Commun.* **2009**, 4521−4523. (g) Velian, A.; Cummins, C. C. *J. Am. Chem. Soc.* **2012**, *134*, 13978−13981.

(9) X = F: Özbolat, A.; von Frantzius, G.; Hoffbauer, W.; Streubel, R. *Dalton Trans.* **2008**, 2674−2676.

(10) X = Cl: Özbolat, A.; von Frantzius, G.; Marinas Pérez, J.; Nieger, M.; Streubel, R. *Angew. Chem.* **2007**, *119*, 9488−9491; *Angew. Chem., Int. Ed.* **2007**, *46*, 9327−9330.

(11) X = Cl: (a) Bode, M.; Daniels, J.; Streubel, R. *Organometallics* **2009**, *28*, 4636−4638. (b) Özbolat-Schön, A.; Ph.D. Thesis, University of Bonn, Bonn, Germany, 2011; (c) Nesterov, V.; Schnakenburg, G.; Espinosa, A.; Streubel, R. *Inorg. Chem.* **2012**, *51*, 12343−12349.

(12) For early attempts, see: (a) Lang, H.; Orama, O.; Huttner, G. *J. Organomet. Chem.* **1985**, *291*, 293−309. (b) Lang, H.; Mohr, G.; Scheidsteger, O.; Huttner, G. *Chem. Ber.* **1985**, *118*, 574−596. (c) Lang, H.; Huttner, G.; Jibril, I. *Z. Naturforsch. B* **1986**, *41*, 473−485. (d) Flynn, K. M.; Olmstead, M. M.; Power, P. P. *J. Am. Chem. Soc.* **1983**, *105*, 2085−2086. (e) Bartlett, R. A.; Rasika Dias, H. V.; Flynn, K. .; Hope, H.; Murray, B. D.; Olmstead, M. M.; Power, P. P. *J. Am. Chem. Soc.* **1987**, *109*, 5693−5698. (f) Jutzi, P.; Kroos, R. *J. Organomet. Chem.* **1990**, *390*, 317−322.

(13) Streubel, R.; Özbolat-Schön, A.; Bode, M.; Daniels, J.; Schnakenburg, G.; Vaca, A.; Pepiol, A.; Farras, P.; Vinas, C.; Teixidor, F. *Organometallics* **2009**, *28*, 6031−6035.

(14) Streubel, R.; Bode, M.; Marinas Pérez, J.; Schnakenburg, G.; Daniels, J.; Jones, P. G. *Z. Anorg. Allg. Chem.* **2009**, *635*, 1163−1171.

(15) Albrecht, C.; Bode, M.; Marinas Pérez, J.; Schnakenburg, G.; Streubel, R. *Dalton Trans.* **2011**, *40*, 2654−2665.

(16) (a) Fankel, S.; Helten, H.; von Frantzius, G.; Schnakenburg, G.; Daniels, J.; Chu, V.; Müller, C.; Streubel, R. *Dalton Trans.* **2010**, *39*, 3472−3481. (b) Fankel, S.; Ph.D. Thesis, University Bonn, Bonn, Germany, 2010; (c) Streubel, R.; Villaba Franco, J. M.; Schnakenburg, G.; Espinosa Ferao, A. *Chem. Commun.* **2012**, *48*, 5986−5988.

(17) (a) Özbolat-Schön, A.; Bode, M.; Schnakenburg, G.; Anoop, A.; van Gastel, M.; Neese, F.; Streubel, R. *Angew. Chem., Int. Ed.* **2010**, *49*, 6894−6898. (b) Nesterov, V.; Özbolat-Schön, A.; Schnakenburg, G.; Shi, L.; Cangönül, A.; van Gastel, M.; Neese, F.; Streubel, R. *Chem.—Asian J.* **2012**, *7*, 845−854.

(18) Streubel, R.; Priemer, S.; Ruthe, F.; Jones, P. G. *Eur. J. Inorg. Chem.* **2000**, 1253−1259.

(19) Khan, A. A.; Wismach, C.; Jones, P. G.; Streubel, R. *Chem. Commun.* **2003**, 2892−2893.

(20) Özbolat, A.; Khan, A. A.; von Frantzius, G.; Nieger, M.; Streubel, R. *Angew. Chem.* **2007**, *119*, 2150−2154; *Angew. Chem., Int. Ed.* **2007**, *46*, 2104−2107.

(21) (a) Streubel, R.; Wilkens, H.; Ostrowski, A.; Neumann, C.; Ruthe, F.; Jones, P. G. *Angew. Chem.* **1997**, *109*, 1549−1550; *Angew. Chem., Int. Ed. Engl.* **1997**, *36*, 1492−1493. (b) Streubel, R.; Ruthe, F.; Jones, P. G. *Eur. J. Inorg. Chem.* **1998**, 571−574.

(22) Gudat, D.; Ph.D. Thesis, University of Bielefeld, Bielefeld, Germany, 1986.

(23) As described in ref 11, but other sterically demanding bases work as well.

(24) This "abnormal" effect was also observed before by Seebach and co-workers in the case of Li/X carbenoids: $\Delta\delta$ = 65.9 between $CHCl_3$ (δ ^{13}C = 80.0) and $CLiCl_3$ (δ ^{13}C = 145.9), $\Delta\delta$ = 142.5 between $CHBr_3$ (δ = ^{13}C 9.7) and $CLiBr_3$ (δ ^{13}C = 152.2), $\Delta\delta$ = 280.0 between CHI_3 (δ ^{13}C = −138.0) and $CLiI_3$ (δ ^{13}C = 142) from Seebach, D.; Siegel, H.; Gabriel, J.; Hässig, R. *Helv. Chim. Acta* **1980**, *63*, 2046−2053.

(25) Marinas Pérez, J.; Klein, M.; Kyri, A.; Schnakenburg, G.; Streubel, R. *Organometallics* **2011**, *30*, 5636−5640.

(26) This hypothesis is strongly supported by the outcome of diffusion measurements on a sample which contained a small amount of unreacted **2a** beside **6a** and allowed thus to determine the value of *D* for both species from the same solution. Analysis of the spectral data confirmed that the difference in diffusion coefficients of both species persists even under these conditions and is thus no artifact but indicates a real deviation in effective molecular size.

(27) Baumgartner, T.; Gudat, D.; Nieger, M.; Niecke, E.; Schiffer, T. J. *J. Am. Chem. Soc.* **1999**, *121*, 5953−5960.

(28) Dransfeld, A.; von Ragué Schleyer, P. *Magnet. Res. Chem* **1998**, *36*, S29−S43.

(29) Compain, C.; Mathey, F. *Z. Anorg. Allg. Chem.* **2006**, *632*, 421−424.

(30) Frisch, M. J.; Trucks, G. W.; Schlegel, H. B.; Scuseria, G. E.; Robb, M. A.; Cheeseman, J. R.; Montgomery, Jr., J. A.; Vreven, T.; Kudin, K. N.; Burant, J. C.; Millam, J. M.; Iyengar, S. S.; Tomasi, J.; Barone, V.; Mennucci, B.; Cossi, M.; Scalmani, G.; Rega, N.; Petersson, G. A.; Nakatsuji, H.; Hada, M.; Ehara, M.; Toyota, K.; Fukuda, R.; Hasegawa, J.; Ishida, M.; Nakajima, T.; Honda, Y.; Kitao, O.; Nakai, H.; Klene, M.; Li, X.; Knox, J. E.; Hratchian, H. P.; Cross, J. B.; Bakken, V.; Adamo, C.; Jaramillo, J. ; Gomperts, R.; Stratmann, R. E.; Yazyev, O.; Austin, A. J.; Cammi, R.; Pomelli, C.; Ochterski, J. W.; Ayala, P. Y.; Morokuma, K.; Voth, G. A. ; Salvador, P.; Dannenberg, J. J.; Zakrzewski, V. G.; Dapprich, S.; Daniels, A. D.; Strain, M. C.; Farkas, O.; Malick, D. K.; Rabuck, A. D.; Raghavachari, K.; Foresman, J. B.; Ortiz, J. V.; Cui, Q.; Baboul, A. G.; Clifford, S.; Cioslowski, J.; Stefanov, B. B.; Liu, G.; Liashenko, A.; Piskorz, P.; Komaromi, I.; Martin, R. L.; Fox, D. J.; Keith, T.; Al-Laham, M. A.; Peng, C. Y.; Nanayakkara, A.; Challacombe, M.; Gill, P. M. W.; Johnson, B.; Chen, W.; Wong, M. W.; Gonzalez, C.; Pople, J. A. *Gaussian 03*, Revision B.02/B.03; Gaussian, Inc.: Wallingford, CT, 2004.

(31) (a) *ADF 2007.01*; Theoretical Chemistry, Vrije Universiteit: Amsterdam, The Netherlands; http://www.scm.com; (b) te Velde, G.;

Baerends, E. J. *J. Comput. Phys.* **1992**, *99*, 84−98. (c) Baerends, E. J.; Ellis, D. E.; Ros, P. *Chem. Phys.* **1973**, *2*, 41−51. (d) Baerends, E. J.; Ros, P. *Chem. Phys.* **1973**, *2*, 52−59.
(32) Becke, A. D. *J. Chem. Phys.* **1993**, *98*, 5648−5652.
(33) Curtiss, L. A.; McGrath, M. P.; Blaudeau, J.-P.; Davis, N. E.; Binning, R. C., Jr.; Radom, L. *J. Chem. Phys.* **1995**, *103*, 6104−6113.
(34) Schaefer, A.; Huber, C.; Ahlrichs, R. *J. Chem. Phys.* **1994**, *100*, 5829−5835.
(35) Krishnan, R.; Blinkley, J. S.; Seeger, R.; Pople, J. A. *J. Chem. Phys.* **1980**, *72*, 650−654.
(36) McLean, A. D.; Chandler, G. S. *J. Chem. Phys.* **1980**, *72*, 5639−5648.
(37) Hay, P. J.; Wadt, W. R. *J. Chem. Phys.* **1985**, *82*, 270−283.
(38) Vosko, S. H.; Wilk, L.; Nusair, M. *Can. J. Phys.* **1980**, *58*, 1200−1211.
(39) Becke, A. D. *Phys. Rev.* **1988**, *38A*, 3098−3100.
(40) Perdew, J. P. *Phys. Rev.* **1986**, *33 B*, 8822−8824. Erratum: Perdew, J. P. *Phys. Rev.* **1986**, *34 B*, 7406−7406.
(41) (a) For Gauge-including atomic orbitals (GIAO), see: Schreckenbach, G.; Ziegler, T. *J. Phys. Chem.* **1995**, *99*, 606−611. (b) For the use of the DFT-GIAO method for ^{31}P and ^{95}Mo NMR calculations, see: Ruiz-Morales, J.; Ziegler, T. *J. Phys. Chem. A* **1998**, *102*, 3970−3976. (c) For ^{183}W NMR calculations, see: Rodriguez-Fortea, A.; Alemany, P.; Ziegler, T. *J. Phys. Chem. A* **1999**, *103*, 8288−8294.
(42) For a comparison of different DFT methods for ^{31}P NMR calculations, see: van Wuellen, C. *Phys. Chem. Chem. Phys.* **2000**, *2*, 2137−2144.
(43) (a) SO ZORA GIAO: Schreckenbach, G.; Ziegler, T. *Int. J. Quantum Chem.* **1997**, *61*, 899−918. (b) For NMR calculations of (neutral) complexes $[(CO)_5W(PX_3)]$ see also earlier work using the ECP/SOS-DFPT approach: Kaupp, M. *Chem. Ber.* **1996**, *129*, 535−544 and ref. cited therein.
(44) Minelli, M.; Enemark, J. H.; Brownlee, R. T. C.; O'Connor, M. J.; Wedd, A. G. *Coord. Chem. Rev.* **1985**, *68*, 169−278.
(45) Pascual-Ahuir, J. L.; Silla, E.; Tunon, I. *J. Comput. Chem.* **1994**, *15*, 1127−1138.
(46) Marenich, A. V.; Cramer, C. J.; Truhlar, D. G. *J. Phys. Chem. B* **2009**, *113*, 6378−6396.
(47) Pyykkö, P.; Atsumi, M. *Chem.—Eur. J.* **2008**, *15*, 186−197.
(48) Rodriguez-Fortea, A.; Alemany, P.; Ziegler, T. *J. Phys. Chem. A* **1999**, *103*, 8288−8294.
(49) Jerschow, A.; Müller, N. *J. Magn. Reson. A* **1996**, *123*, 222−225. Jerschow, A.; Müller, N. *J. Magn. Reson. A* **1997**, *125*, 372−375.
(50) (a) Fischer, E. O.; Kollmeier, H. J. *Chem. Ber.* **1971**, *104*, 1339−1346. (b) Bodner, G. M.; Kahl, S. B.; Bork, K.; Storhoff, B. N.; Wuller, J. E.; Todd, L. J. *Inorg. Chem.* **1973**, *12*, 1071−1074 , and literature cited therein.
(51) Dötz, K. H. *Chem. Ber.* **1980**, *113*, 3597−3604.
(52) (a) Appel, R.; Westerhaus, A. *Tetrahedron Lett.* **1981**, *22*, 2159−2160. (b) Issleib, K.; Schmidt, M.; Wirkner, C. *Z. Chem.* **1981**, *21*, 357−358.